Computer Networks 253 (2024) 110726

Contents lists available at ScienceDirect

Computer Networks

journal homepage: www.elsevier.com/locate/comnet

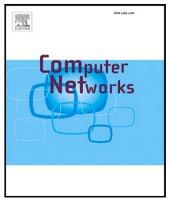

# Integrating terrestrial and non-terrestrial networks via IAB technology: System-level design and evaluation

Daniele Pugliese [a,b,*], Mattia Quadrini [d], Domenico Striccoli [a,b], Cesare Roseti [c], Francesco Zampognaro [e], Giuseppe Piro [a,b], Luigi Alfredo Grieco [a,b], Gennaro Boggia [a,b]

[a] Department of Electrical and Information Engineering, Politecnico di Bari, Bari, Italy
[b] CNIT, Consorzio Nazionale Interuniversitario per le Telecomunicazioni, Italy
[c] Department of Electronic Engineering, Universita' di Roma "Tor Vergata", Roma, Italy
[d] Research and Development, RomARS S.r.l., Rome, Italy
[e] Department of Human Sciences, Link Campus University, Rome, Italy

ARTICLE INFO

*Keywords:*
Non-terrestrial networks
Satellite communications
Integrated access-backhaul
Architectural analysis
Sixth-generation
System-level simulator

ABSTRACT

As the telecommunications industry embarks on the transition to Sixth-Generation (6G) networks, this paper examines the integration of Non-Terrestrial Networks (NTN), and in particular satellite backhauling, in the context of Fifth-Generation (5G) systems. The Integrated Access and Backhaul (IAB) technology, conceived as a wireless terrestrial backhauling system in the Next Generation Radio Access Network (NG-RAN), has been identified as a possible enabler for the integration of satellite nodes. Despite the work already done in this direction, the combination of IAB architectures with satellite nodes operating in both the access and backhaul side requires further evaluations on feasibility and limitations for networks integrating Low Earth Orbit (LEO) and Geostationary Earth Orbit (GEO) satellites. To this end, this work contributes providing insights on background technologies, as well as a detailed analysis of the issues and challenges arising from such integration and a definition of use cases to support narrow-band and broadband services. Furthermore, the design and implementation of a simulation tool is proposed for a performance evaluation in terms of registration time, link capacity, single-hop and end-to-end delay. Results show that the integration turns out to be feasible, even if with strong constraints coming from the satellite system rather than the IAB usage itself. Indeed, the earth-satellite link in LEO systems has a significant impact on the packet delivery time due to the discontinuous coverage. In case of GEO satellite instead, a non-terrestrial backhaul link could limit the performance of the whole system, especially at lower elevation angles.

## 1. Introduction

In recent years, the use of Non-Terrestrial Networks (NTN), and Satellite Communication (SatCom) systems in particular, has become increasingly popular, paving the way for previously unexplored scenarios. Such platforms offer significant advantages for the next generation of mobile services, such as wide area coverage and significantly reduced vulnerability to physical attacks or natural disasters [1]. The interest in this new architectural paradigm is also evident in the latest Third Generation Partnership Project (3GPP) releases, which include new reports and specifications to extend Next Generation Radio Access Network (NG-RAN) with NTN [2,3]. At the same time, the goal of wider coverage has led to increased attention on wireless backhauling systems, known as Integrated Access Backhaul (IAB), as an essential complementary solution for sites where fiber is either unavailable or cost-prohibitive [4]. Adopting satellite nodes is the direction to follow, in order to achieve what, in the vision behind Sixth-Generation (6G), is defined as ubiquitous coverage and a three-dimensional network [5]. However, the current solutions proposed by 3GPP for this integration do not follow standardized guidelines (e.g. regenerative relaying, transparent relaying), leaving the implementation of such solutions to the industry [6]. This integration, therefore, can benefit from the use of IAB technology, thanks to which a large number of terrestrial and satellite nodes can be deployed with minimal effort in terms of configuration [7]. There are many possible topologies that can be realized based on this freedom in terms of set-up, although the problems and limitations introduced should not be neglected. Regarding the ground-to-space link, the use of a Low Earth Orbit (LEO) satellite rather than a Geostationary Earth Orbit (GEO) satellite introduces the uncertainty of link availability for the former, and high delays and attenuation for the

* Corresponding author at: Department of Electrical and Information Engineering, Politecnico di Bari, Bari, Italy.
*E-mail address:* daniele.pugliese@poliba.it (D. Pugliese).

https://doi.org/10.1016/j.comnet.2024.110726
Received 15 March 2024; Received in revised form 26 June 2024; Accepted 18 August 2024
Available online 22 August 2024

latter [8]. With regard to the standardized Fifth-Generation (5G) NG-RAN, based on the satellite platform used, some adaptations at different layers of the protocol stack are required to address the introduced issues. They include the extended delivery time, which affects the normal Hybrid Automatic Repeat reQuest (HARQ) and Random Access CHannel (RACH) procedures, as well as high Doppler shifts (in the case of LEO satellites), for which pre- and post-compensation techniques are required [9]. Constraints must also be considered in terms of resources, both with regard to the band that can be used (e.g. S-Band or Ka-Band), and also to the distribution in the capacity of the wireless link between access and backhaul.

Given the above-mentioned complex, yet fascinating scenario arising from the integration of NTN in IAB architectures, there is the need to contribute to the scientific efforts aiming to study the applicability and feasibility of IAB architectures in which satellite links feed both the access and backhaul. Also, it is very important to analyze the connectivity performance of the satellite link in such architectures, for both LEO and GEO satellites, while taking into account the most recent 5G specifications. Finally, it would be desirable to apply the study on the satellite link in a multi-user system, testing some key performance metrics through an intensive simulation campaign in some representative use cases.

This work aims to satisfy these needs by contributing in three directions: First, it provides an insight into the background of NG-RAN, IAB technology and NTN. It also presents a detailed analysis of the issues and challenges arising from the integration of NTN and IAB components, and proposes some representative network topologies; Second, it proposes a simulation platform, tailored for integrated NTN-IAB systems, describing its main design and implementation details, including the analysis of the satellite link characteristics (i.e., satellite movement, link budget, block error rate, etc.) that allow evaluating its connectivity performance for both LEO and GEO satellites; Third, it shows simulation results on key performance metrics like registration time, link capacity, single hop and end-to-end delay in two representative use cases. The latter are computed exploiting the implemented platform to understand the applicability and limitations of the NTN-IAB networks in practical scenarios of interest.

The remainder of the present work is structured as follows: Section 2 motivates the need to evaluate solutions that integrate NTN via IAB, highlighting the added contribution of this work in comparison to related works, as well as the underlying technologies behind it. Section 3 provides an overview of the issues linked to IAB NTN architectures, examines some promising topologies and describes the studied use cases. Section 4 gives an in-depth explanation of how the simulation platform has been realized, from the modeling of the satellite link to the implementation of the IAB node. Section 5 analyzes from a performance point of view the use cases chosen for the study. Finally, Section 6 concludes the work giving future investigation directions[1].

## 2. Background and motivation

The integration of NTN via IAB is emerging as a crucial topic of interest in the field of mobile networks. With the rapid evolution of technology and the growing need for enhanced wireless connectivity, many contributions are exploring this topic and analyzing different points of view. For instance, authors in [10] propose an efficient IAB architecture for integrated satellite-terrestrial networks based on reverse Time Division Duplex (TDD) considering both uplink and downlink. The offered solution helps in preventing, with the cooperation of the 5G Node B (gNB), both self-interference and interference between access links and backhaul links. Moreover, such a architecture is verified using the channel models defined by the 3GPP. Definitively, numerical results show that the proposed architecture significantly improve performance

**Table 1**
List of acronyms.

| Acronym | Full text |
|---|---|
| 3GPP | Third Generation Partnership Project |
| 5G | Fifth-Generation |
| 5GC | 5G Core |
| 5GS | 5G System |
| 6G | Sixth-Generation |
| AMC | Adaptive Modulation and Coding |
| AMF | Access and Mobility Management Function |
| AN | Access Network |
| BAP | Backhaul Adaption Protocol |
| BLER | BLock Error Rate |
| BS | Base Station |
| CBR | Constant BitRate |
| CQI | Channel Quality Indicator |
| CU | Central Unit |
| CU-CP | CU-Control Plane |
| CU-UP | CU-User Plane |
| DCF | Diagram Correction Factor |
| DU | Distributed Unit |
| EIRP | Equivalent Isotropically Radiated Power |
| FDD | Frequency Division Duplex |
| FR1 | Frequency Region 1 |
| FR2 | Frequency Region 2 |
| FSPL | Free Space Path Loss |
| FSS | Fixed Satellite Service |
| FTP | File Transfer Protocol |
| FWA | Fixed Wireless Access |
| GEO | Geostationary Orbit |
| gNB | 5G Node B |
| GSO | Geostationary Satellite Orbit |
| HAPS | High Altitude Platform Stations |
| HARQ | Hybrid Automatic Repeat reQuest |
| HEO | Highly Elliptical Orbit |
| HLS | Higher Layer Split |
| IAB | Integrated Access Backhaul |
| IoT | Internet of Things |
| ISL | Inter-Satellite Link |
| KPI | Key Performance Indicator |
| LB | Link Budget |
| LEO | Low Earth Orbit |
| LLS | Lower Layer Split |
| LTE | Long Term Evolution |
| MAC | Media Access Control |
| MCS | Modulation and Coding Scheme |
| MIESM | Mutual Information Effective SNR Mapping |
| MNO | Mobile Network Operator |
| MT | Mobile Termination |
| NAS | Non Access Stratum |
| NG | Next Generation |
| NG-RAN | Next Generation Radio Access Network |
| NGSO | Non-Geostationary Orbit |
| NOMA | Non Orthogonal Multiple Access |
| NR | New Radio |
| NTN | Non Terrestrial Networks |
| O-RAN | Open RAN |
| OFDM | Orthogonal Frequency Division Multiplexing |
| PDCP | Packet Data Convergence Protocol |
| PDU | Protocol Data Unit |
| PHY | Physical Layer |
| PLR | Packet Loss Ratio |
| PSD | Power Spectrum Density |
| QoS | Quality of Service |
| RACH | Random Access CHannel |
| RAN | Radio Access Network |
| RB | Resource Block |
| RE | Resource Element |
| RLC | Radio Link Control |
| RRC | Radio Resource Control |
| SAN | Satellite Access Node |
| SatCom | Satellite Communication |
| SCS | Sub Carrier Spacing |
| SDAP | Service Data Adaptation Protocol |
| SINR | Signal to Interference plus Nois Ratio |

(*continued on next page*)

[1] For a complete list of acronyms used in this work, see Table 1.

**Table 1** (*continued*).

| | |
|---|---|
| SNR | Signal to Noise Ratio |
| TA | Timing Advance |
| TB | Transport Block |
| TBS | Transport Block Size |
| TDD | Time Division Duplex |
| TS | Technical Specification |
| UAV | Unmanned Aerial Vehicle |
| UC1 | Use Case |
| UC2 | Use Case |
| UE | User Equipment |
| UPF | User Plane Function |
| VoIP | Voice over IP |
| VSAT | Very Small Aperture |

with respect to the classical out-of-band backhauling, while approaching an outer bound of the uplink–downlink rate region. Authors in [11] instead, evaluate the adoption of extended Non Orthogonal Multiple Access (NOMA) protocol, namely NOMA Coordinated Direct and Relay Transmission, in IAB networks to implement data relaying and mitigate interference issues. The communication is managed in two phases using an half-duplex approach. Terminals in direct access are able to recover their signal combining transmissions propagated in both phases. NOMA operates at Media Access Control (MAC) layer and allows an improve of the data rate. Moreover, authors in [12] investigate the adoption of base stations mounted on board Unmanned Aerial Vehicle (UAV) to implement an IAB network. The objective is to exploit opportunistically these links to relay user data in the backhaul. The analysis on the feasibility highlights how the velocity of the aerial platforms impact on the coverage and handover probabilities. Finally, authors in [13] evaluate the possibility to use High Altitude Platform Stations (HAPS) to expand the coverage of a Radio Access Network (RAN) implementing IAB. In particular they analyze the available bandwidth (downlink and uplink) provided to each HAPS station depending on the position with respect to the donor. They use a common stochastic geometry models to model a IAB network. They conclude that HAPS greatly provide an extension of the coverage region. In particular, overall network performance improves in areas with high demand for high-speed data, such as hotspots, by avoiding network congestion. Nevertheless, dividing resources efficiently or using NOMA to achieve a sharper separation requires a simulation platform where such solutions can also be implemented in satellite scenarios. Satellites that, compared to UAVs and HAPSs, have several limitations due to which assessing the type of service that can be offered requires a detailed design phase. With this in mind, the analysis continues assessing what underlies the use of such a integrated system. These recently published contributions demonstrate the interest in integrating non-terrestrial nodes through IAB and optimizing the division of radio resources shared with backhauling.

### 2.1. NG-RAN overview

The NG-RAN [3] consists of one or more gNB providing User Equipments (UEs) with a wireless access to the 5G Core (5GC). The gNB serves the UE devices under coverage, via the New Radio (NR) interface in the Access Network (AN), and forward Control and User plane data to the 5GC in the backhaul network over N2 to the Access and Mobility Management Function (AMF), and towards N3 to the User Plane Function (UPF) (i.e. NG interfaces). For the scope, the gNB implements a dual protocol stack. The analysis carried out in this paper focuses on the NR protocol stack, which consists of: Physical Layer (PHY), MAC, Radio Link Control (RLC), Packet Data Convergence Protocol (PDCP), Radio Resource Control (RRC), Service Data Adaptation Protocol (SDAP), and Non Access Stratum (NAS).

The NG-RAN architecture can be centralized (a single gNB) or distributed [14], i.e., a set of Distributed Units (DUs) and a Central Unit (CU) represents the logical gNB. The DU interacts directly with the UE in the AN, while the CU control several DUs over F1 interfaces (i.e., F1-C and F1-U for control and user planes, respectively). In addition, the user plane and control plane functions of the CU can be split obtaining the CU-User Plane (CU-UP) and CU-Control Plane (CU-CP), respectively. These latter communicate among themselves over the E1 interface. Multiple and different splitting options have been analyzed in the 3GPP study 38.801 [14] and grouped as in Fig. 1. Higher Layer Split (HLS) relates to options 1–5, while Lower Layer Split (LLS) to options 6–8. The Option 8 represents the separation between the physical radio unit from the logical part of the gNB. By the way, constraints and limitations must be considered and evaluated at different layers as addressed in the whitepaper [15]. The splitting Option 2 adopted by 3GPP presents a latency for the communications between RLC (at DU) and PDCP (at CU) in the order of a few milliseconds (<5 ms), as illustrated in Fig. 1. The figure also reports the maximum supported data rate and distance which correspond to 10 Gbit/s and 100–400 km respectively (Option 2). The reported values are tailored assuming a wired connectivity (i.e., fiber), thus the possible extension to wireless midhaul/backhaul needs a review. In fact, delay and bandwidth constraints must be re-adapted for the link budget purposes, especially when considering NTN (e.g., Satellite domain).

### 2.2. Integrated Access-Backhaul

The IAB is defined by the 3GPP for the 5G-NR technology starting from Release 16 [16] and then in Release 17 [3]. The IAB consists of relaying the UE data in the backhaul, using a wireless link. This working principle is not new, rather is already proposed in Long Term Evolution (LTE) (Rel10) known as "LTE relaying". Nonetheless, spectrum requirements did not allow the wise use of this function, making this technology not interesting from a commercial point of view.

The IAB architecture as well as the protocol stack are illustrated in Fig. 2 leveraging the gNB CU/DU splitting architecture. The set of IAB-donor (or simply donor) and IAB-node(s) (or simply node) compose the gNB. At least one donor and one node are required. The donor is the element closest to the 5GC. It implements both DU (donor-DU) and CU (donor-CU) functionalities. The donor-CU interfaces to the 5GC over the N2 and to both the other donor-DU and IAB-node elements over the F1 interface. Eventually, the Xn interface allows communication with neighboring gNB. The node handles the UE communication on the NR-Uu interface and relays the UE data towards either the parent node or the donor. The node implements the DU functionalities and is controlled by the donor-CU over F1 interface. Eventually, the F1 traffic from the node to the donor can be managed by intermediate nodes, using dedicated protocols. The node is also provided with a subset of UE functionalities which are used to forward data in the backhaul. This is referred to the IAB-Mobile Termination (MT) (or simply MT). IAB-MT implements Layer-2 protocols including PDCP, RRC and NAS required to perform some initial signaling and management operations (see bottom of Fig. 2). As a matter of fact, the IAB-node acts as a "gNB" from the UE's perspective in the access network (i.e., DU), and as a "UE" towards the following IAB element in the backhaul (i.e., MT). By the way, an adaptation layer, the Backhaul Adaption Protocol (BAP) [17], is required to manage traffic in the backhaul as well as to provide Quality of Service (QoS) management and routing operation. For the scope, dedicated backhaul network RLC channels are defined between two adjacent nodes and with the donor, in order to guarantee a target QoS level and traffic prioritization. The donor-DU terminates every BAP communication. Once the BAP header is removed, IP packets containing user plane data (i.e., GTP-U packets) are processed and forwarded to the donor-CU where GTP tunnels are terminated.

The IAB topology consists of *parent* and *child* nodes. The parent node is the node located towards the donor (i.e., the Upstream), while the child node is the node in the opposite direction (i.e., the Downstream). The IAB topology could be set up with multiple paths,

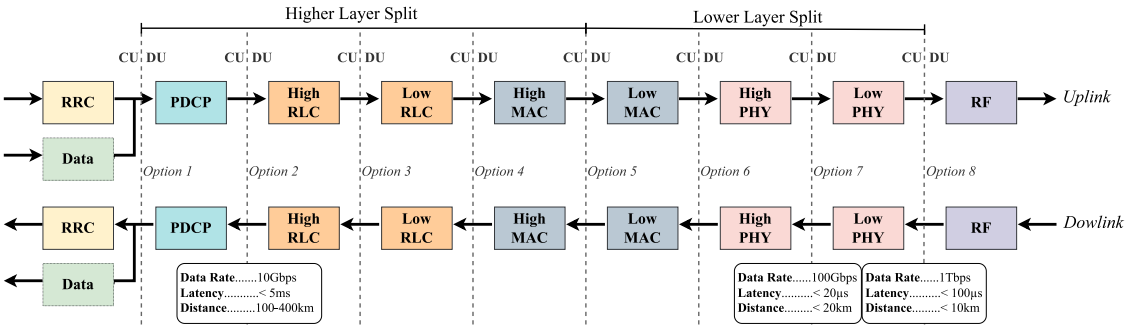


**Fig. 1.** CU/DU identified splitting options in [14].

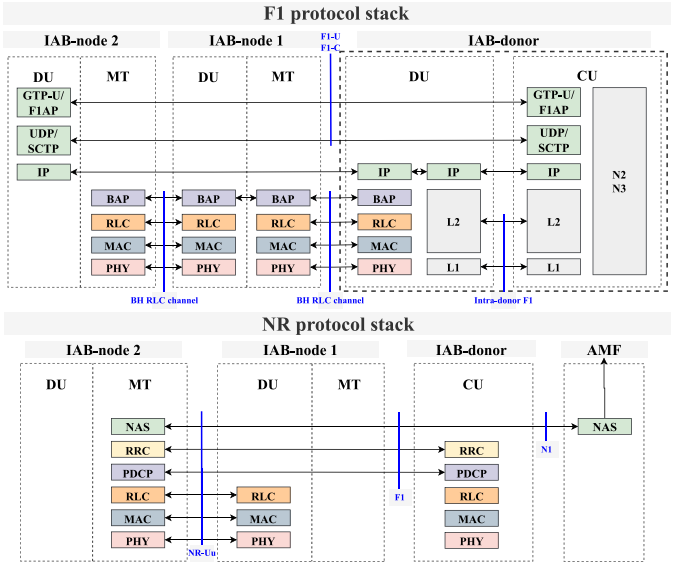


**Fig. 2.** The IAB architecture and protocol stack. In the F1 protocol stack (top) UDP/GTP-U and SCTP/F1-AP refer to the user and control plane respectively.

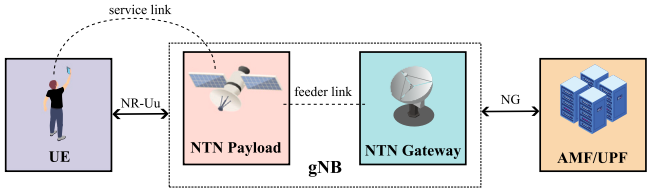


**Fig. 3.** Overall illustration of an NTN-RAN.

managed by different nodes. For each path, multiple backhaul network links are established. Path redundancy can be configured to guarantee resiliency to link interruptions. Definitively, for each node at least six links shall be considered, such as a pair of uplink/downlink for the Upstream/Downstream in the backhaul, and a pair of uplink and downlink towards the UE in the access.

The IAB transmission and receptions aspects are defined in the Technical Specification (TS) document number 38.174 [18]. The set of frequencies for IAB service are defined both in the Frequency Region 1 (FR1) (i.e., 410–7125 MHz) and Frequency Region 2 (FR2) (i.e., 24 250–71 000 MHz) using TDD scheme. Two operational modes are specified: the In-Band and the Out-of-Band. The former allows to reuse the same frequency band for the access and backhaul transmissions, creating total or partial overlaps. Therefore, interference constraints are introduced, limiting the simultaneous transmission and reception operations of the node on both links. The latter overcomes overlapping and then interference constraints by separating in the frequency domain the access and backhaul resources. Transmission and reception operations towards child and parent nodes shall be scheduled among access and backhaul networks. In general, the DU and MT parts of an IAB-node cannot operate simultaneously, unless they are exploiting spatial multiplexing capabilities. Then, the donor-CU is in charge to configure the served DUs. The resource configuration consists of a set of symbols indicating if a transmission or a reception can occur, can be scheduled, or cannot be executed. Accordingly, three possible values can be assigned:

- Hard (H) – a transmission and reception can occur;
- Soft (S) – a transmission or a reception can be scheduled with a condition, i.e., based on the explicit indication by the parent IAB-nodes or the implicit determination of the availability by the same IAB-node (which will consider if the DU transmission has an impact on the transmission of the MT);
- Unavailable (U) – the transmission or reception cannot occur, except for some special cases.

To facilitate transitioning from backhaul to access operation and vice versa, guard symbols (G) can be used to overcome potentially misaligned symbol boundaries. The IAB-node can indicate to a parent node a number of desired guard symbols, while the parent node can indicate to the IAB-node the number of actually provided guard symbols for specific transitions. This operation facilitates the transmission and reception operations between DU and MT of adjacent nodes.

### 2.3. Non-Terrestrial Networks

3GPP defined the support to NTN since Release 16, in particular proposed two Technical Reports (TR), the number 38.811 [19] and the number 38.821 [6], by identifying issues and possible solutions for NTN deployments. The word "Non-Terrestrial Network" is used by the 3GPP to identify those communication scenarios at an altitude higher than 10 km such as: aeroplanes, HAPS, and satellites. Starting from Release-17 [3], the 3GPP approved the introduction of NTN to provide non-terrestrial NR access via the NTN Gateway and the NTN Payload. The latter refers to the Satellite Access Node (SAN) as specified in [20]. Fig. 3 illustrates the overall architecture of a NTN-RAN. Two SAN classes are defined: the LEO class assuming LEO constellation at 600 km and 1200 km of altitudes; the GEO class assuming GEO constellation at 35 786 km of altitude. The frequency spectrum allocation for SAN is defined in the FR1 (Rel-17) and counts two operating frequencies in the L/S band using Frequency Division Duplex (FDD) mode: the frequency band number n256 (i.e., 1980–2010 MHz for Uplink and 2170–2200 MHz for Downlink), and the frequency band number n255 (i.e., 1626.5-1660.5 MHz for Uplink and 1525–1559 MHz for Downlink).

## 3. Architectural analysis

IAB technology has been defined considering terrestrial wireless requirements which differs from those for SatCom (e.g., delay, link budget, available capacity). Therefore, the design of an NTN-IAB architecture requires the analysis of NTN issues and possible adaptations at protocol and system layers.

### 3.1. Issues and challenges

Issues occur at different levels, such as the satellite system architecture, frequency selection and bandwidth management, as well as transmission management. The subsequent analysis focuses on the seamless integration of the NTN component within an IAB network. The impact of various aspects is contingent upon the specific configuration of the NTN system, including factors such as service types (e.g. from broadband services, including voice and data applications, to narrowband services for sensors and smart objects), the classification of target terminals (e.g. handheld, fixed, wearable, or sensor/actuator), the spatial extent of service coverage, and the satellite payload characteristics (e.g. transparent or regenerative with on board processing.

The design of the satellite system architecture is a crucial factor influencing both service provision and target terminals. Satellite orbit selection delineates two main architectures. The former takes advantage on GEO satellites, characterized by a persistent link to the NTN Gateway. These satellites, operating at higher altitudes, provide extensive coverage and facilitate direct connections with ground-based IAB elements and even the 5GC. For broadband services demanding high data rates, this scenario is particularly well-suited for fixed access terminals employing Very Small Aperture (VSAT) antennas. These latter provide focused signal strength and longer communication ranges compared to omnidirectional ones, enhancing signal robustness and consequently the maximum achievable datarate. An example is the Fixed Wireless Access (FWA) technology commonly deployed for residential or commercial Internet access. However, it is worth noting that handheld terminals can also be accommodated, albeit with a reduced link capacity, primarily serving voice applications. The latter architecture leverages on LEO satellites, providing time-limited IAB services. LEO satellites facilitate direct access to handheld terminals, achieving higher data rates compared to the previous scenario. However, this advantage comes with a trade-off, i.e., the visibility time due to specific orbit characteristics. Therefore, the satellite link is available only during limited time slots. For global and continuous coverage, a full constellation of satellites has to be designed to ensure service continuity. Consequently, efficient satellite handover procedures must be implemented, and Inter-Satellite Link (ISL) may be necessary to optimize traffic routing along an IAB path towards the donor. Note that the reachability of the NTN Gateway is a critical requirement for NTN-IAB, which can be met by: (i) assuming a distributed network of NTN Gateways near UE devices and extending the interval of simultaneous coverage using a single Non-Geostationary Orbit (NGSO) satellite (with a terrestrial connection between the NTN Gateway and the 5GC); (ii) considering onboard installation of both donors and user plane components on the satellite to support store-and-forward mechanisms. However, by installing multiple NTN Gateways may not be feasible due to cost and scalability constraints, making option (i) less viable. In the case of a satellite serving as an IAB-donor, the IAB topology loses consistency, effectively configuring the satellite as a full RAN with local traffic breakout capabilities, which falls outside the scope of traditional IAB configurations.

The selection of frequency and management of bandwidth are intrinsically linked. It is worth noting that the current set of frequency bands delineated for SAN are not in compliance with those reserved for IAB. Furthermore, SANs are projected to operate in FDD, in contrast to IAB, which has been standardized to operate in TDD as of the current 3GPP release. Upon adopting the In-Band configuration, the selection of frequencies is confined to those defined in the L/S band exclusively, in order to meet the requirements of handheld devices, such as dimensions, antenna size, costs, and complexity. The In-Band configuration is advocated for NGSO satellites or in scenarios where Geostationary Satellite Orbit (GSO) support fixed and wideband access. In the case of Out-of-Band, the selection of frequencies can be expanded to include those defined for Fixed Satellite Service (FSS), such as K/Ka/Ku or Q/V bands, which support backhaul communications towards other satellites (via ISL) or ground stations [21,22].

Given an In-Band configuration, the downstream and upstream transmission requires strict coordination. This coordination is initially spearheaded by the donor implementing the CU, and subsequently propagated to the other nodes, which are in turn influenced by the configuration of the adjacent node. As previously discussed in Section 2.2, distinct transmission phases can be delineated for the downlink and uplink to optimize the node switching operations in a half-duplex mode. Specifically, contingent on the role (node or donor) of the satellite, the transmissions of the node within the coverage will be obstructed due to interference constraints. If the satellite node is transmitting in both the access and backhaul or solely in the access, all other stations within the coverage are prohibited from downlink transmissions.

### 3.2. Satellite IAB topologies

An IAB network, by definition, can encompass multiple nodes that support a diverse range of topologies. As highlighted in Ericsson's review [4], certain characteristics that make the IAB unique can conversely diminish the actual size of the network, particularly in relation to the In-Band configuration. It is important to underscore that as the number of nodes escalates, the backhaul capacity required for a single node correspondingly increases. Indeed, the link capacity of a node must be adequate to accommodate both the information of the UEs being served in the AN and that of the child nodes in the backhaul. Consequently, a multi-hop topology could instigate congestion at the network level, potentially as early as the first hop. The exploitation of the satellite can mitigate the dimension and load of the IAB network, as the node can potentially establish connection with the donor via a single hop, thereby bypassing the terrestrial nodes. In the following, various satellite topology options are presented, wherein the satellite (represented by the gray circle in Fig. 4) hosts an IAB-node or a donor while interacting with terrestrial IAB elements (depicted as orange circles). The first two options, namely *(a)* and *(b)* in Fig. 4, refer to the satellite IAB-node, while the option *(c)* refers to the satellite IAB-donor, and the last option *(d)* assumes a fully satellite IAB network. As first consideration, note that requirements at PDCP layer (i.e., buffering packets and timers) are different for all the options aforementioned. For a satellite IAB-node, PDCP connections are closed at the ground donor-CU, experiencing a doubled latency due to the transmission between the terrestrial and orbital stations. On the contrary, for a satellite IAB-donor, PDCP connections are closed on board the satellite by experiencing only one satellite delay.

In the topology option *(a)*, a single satellite implements the IAB-node protocol stack, thereby serving as the final hop to establish connectivity with the terrestrial donor. This satellite essentially oversees the backhauling from child nodes to the terrestrial donor. The BAP at the ground nodes is configured to route data to the satellite by default in order to reach the donor in the upstream direction (i.e., static routing). Similarly, the BAP at the donor is configured to forward all backhaul traffic to the satellite for downstream communication. It is essential to ensure continuous connectivity between the donor and the nodes over time to guarantee an uninterrupted service. This can be particularly critical in the case of LEO orbits, but is not a concern for GEO and Highly Elliptical Orbit (HEO) platforms. In such a configuration, the satellite IAB-node can be directly accessed by NTN UE terminals, thereby extending the range of supported operational scenarios. This topology provides the flexibility to deploy the donor in

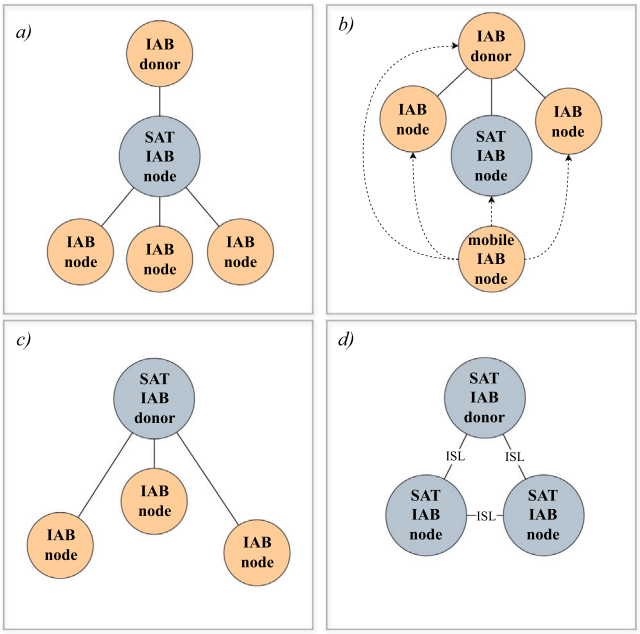


**Fig. 4.** Satellite IAB topology options. (For interpretation of the references to color in this figure legend, the reader is referred to the web version of this article.)

close proximity to the 5GC, which has the potential to reduce latency on Next Generation (NG) interfaces and also decrease the number of required terrestrial nodes. Without loss of generality, the IAB-donor can be situated within the terrestrial Mobile Network Operator (MNO) premises, allowing for direct action on the control plane. However, it is important to note that the satellite still represents a bottleneck in terms of capacity (i.e., number of served terminals, whether UEs or nodes) and end-to-end delay (e.g., re-transmissions due to adverse weather conditions).

In a different configuration, the IAB-node represents an additional path to reach the donor on the ground, as addressed in option *(b)*. The SatCom can be exploited opportunistically when a mobile IAB-node (on the ground) cannot be served by either terrestrial IAB-node or IAB-donor (out of coverage). The BAP plays an important role by coordinating handover activities between terrestrial and satellite links. Similar scenarios are presented in the 3GPP report 22.839 [23] where mobile vehicular relays are assumed moving to an area uncovered by terrestrial RAN. The satellite link capacity requirement is statistically lower with respect to the previous case as the satellite is serving occasionally in the backhaul.

The satellite takes a different role in the topology option *(c)* by implementing IAB-donor to serve both child IAB-nodes and UE terminals on the ground. This option assumes the MT protocol stack on board is no longer required, while it is replaced by CU. The connectivity towards the 5GC is provided by the satellite via the NTN Gateway (i.e., feeder link). Therefore NG interfaces (i.e., N2/N3) must be exposed over the Satellite Radio Interface (SRI). Note that, in some scenarios where a satellite constellation is required, one can consider the deployment of multiple IAB-donors (i.e., one per satellite). Accordingly, the 3GPP specification 38.401 [24] defines this possibility to guarantee resiliency (i.e., a single DU is registered to many CUs). Definitively, the IAB domain terminates at the satellite, leaving the possibility to adopt SatCom legacy technology to manage communication on the feeder link to the ground. Although, the experienced latency in the RAN is halved with respect to have the IAB-node onboard, some constraints must be accounted. The MNO is expected to have some knowledge of the SatCom infrastructure, as well the access to the satellite payload must be guaranteed to manage control plane functions (e.g., configuration, upgrade, updates).

The last option *(d)* proposes a full satellite IAB system. The IAB network is fully deployed on a satellite constellation including IAB-nodes and donor. As a matter of fact, this option merges all other previous options, resulting to have an equivalent gNB on the space potentially covering users spread worldwide. Therefore, the design of the IAB system can overcome 3GPP constraints in terms of frequency bands and duplexing scheme. Concerning the routing at BAP layer, this could be either static or based on preconfigured policies since the topology is predictable at any time and the available bandwidth allows to avoid load balancing problems. Some drawbacks are identified: the support to ISL is mandatory; the latency experienced at the PDCP layer is high and time-varying (routing could changes) with respect to previous topologies; last, the IAB support covers only NTN UE terminals.

### 3.3. Architecture selection and use cases

The analysis conducted so far provides a technical baseline to integrate SatCom into a IAB network, drawing the main issues and potentialities. At a first glance, taking into account the wide satellite coverage and the constraint about the IAB network size in a real-world scenario, the viable satellite topology options can be reduced to options *(a)*, *(b)* and *(c)* referring to an "hybrid terrestrial-satellite" approach, where IAB elements are spread over both the terrestrial and the satellite domain. This latter is covered in this work and provides the two main architectures discussed in the following.

The first architecture assumes the satellite IAB-node (i.e., option *(a)*). Because the IAB-nodes implement also the MTs part (i.e., they act as UE in the backhaul), they require link level adaptations provided in the "NTN Config" defined in the TS 38.331 [25]. This latter is sent to the device using RRC signaling (i.e., SIB19) and contains different level of information such as: *EphemerisInfo* (i.e., satellite ephemeris either in format of position and velocity state vector or in format of orbital parameters); *epochTime* (i.e., the epoch time for the NTN assistance information); *ntn-PolarizationUL/DL* (i.e., polarization information for uplink/downlink transmission on service link, including Right hand, Left hand circular polarizations and Linear polarization); *ntn-UlSyncValidityDuration* (i.e., a validity duration configured by the network for assistance information); *ta-Common* (i.e., network-controlled common Timing Advance (TA) value and it may include any timing offset considered necessary by the network); *ta-Report* (i.e., it indicates reporting of TA is enabled during Random Access due to RRC connection establishment or RRC connection resume, and during RRC connection reestablishment). As well, also UE devices served by terrestrial nodes require to be configured to work with satellite latencies since PDCP connections are crossing space platforms to reach the donor. Such custom configurations shall be coordinated and distributed by the donor-CU which shall be aware of the satellite link. Concerning the design of the satellite system, i.e., the selection of the orbital and operating frequency bands, has an impact on the service scenario, as discussed below. NGSO satellites greatly relaxes the link budget requirements allowing communications with commercial UE terminals equipped with small-sized antennas. The NTN adaptations currently limit the achievable data-rate (i.e., few hundreds kbit/s as reported in a previous study [9]), thus reducing the number of services offered via the IAB system, such as sensor networks and Internet of Things (IoT). As mentioned before, NGSO introduces a visibility time issue. Then, both NTN UEs and ground IAB-nodes "see" the orbiting satellite for a few minutes. Within this window, the CU signaling and registration procedures must be successfully concluded with the IAB-donor and the 5GC, respectively. Considering satellite delays, such a setup time is not negligible, further narrowing the actual time to transmit application data resulting in a severe constraint for the application. With the resulting framework, the configuration of a single NGSO satellite enhanced with IAB-node interfaces is deemed of interest for a large-scale network of 5G NTN-capable sensors and IAB-nodes covering 5G

sensors with an IAB configuration fully compliant to the current 3GPP specifications: L/S band (i.e., in the IAB FR1 spectrum range), TDD duplexing scheme, and In-Band configuration. This configuration sets up the Use Case 1 (UC1) supporting the communication in a sensor network and IoT scenario, as illustrated in Fig. 5. The message exchange is not very frequent, while the uplink transmission requires a small amount of bandwidth and time. The satellite serves a wide area to collect measurements in an agriculture environment ("NTN Sensors"). The deployment of a low-cost terrestrial node can further extend NG-RAN coverage adding the support also to ground sensors ("Sensors") in the access network. As well, the IAB-donor will serve other ground sensors present in the coverage while processing forwarded data to the 5GC.

The latter covered architecture assumes a IAB-donor equipped on board the satellite. All communications are managed by the DU part: in the backhaul towards ground IAB-nodes; in the access towards NTN UEs. Note that, the same NTN NR protocol stack is used, and the satellite acts always as "the gNB". In fact, this latter must handle connectivity to AMF and UPF in the 5GC by exposing the N2 and N3 interfaces accordingly. The IP communication to the core network is in charge of the CU part and is supported by the NTN Gateway by leveraging satellite technology out of the IAB perimeter. PDCP connections terminate on board the satellite, thus halving the satellite latency in the access with respect the previous architecture. The IAB-donor on board the satellite is particularly attractive to represent an anchor for possible IAB-nodes to be installed on demand to create cost-effective 5G bubbles. In this view, GSO is a compelling choice to maximize the effective operational area. As a drawback, more critical physical constraints narrow the service to a FWA, with hardware and antenna technologies able to compensate the harsh communication conditions. Frequencies belonging to IAB FR2 spectrum range are recommended in this scenario. In fact, with respect to the previous scenario, the satellite could handle a larger amount of traffic to/from the 5GC since the backhaul multiplexes traffic coming from several access networks (i.e, IAB-nodes). Nevertheless, operating frequency bands in the IAB FR2 are not yet defined for SAN [20], then in this work only IAB FR1 is considered. This scenario can generate potential use-cases of interest involving GSO and adopting FDD scheme in combination with Out-of-Band configuration. The FDD scheme is recommended to tailor the link between satellite and NTN Gateway with consolidated satellite technology available in the market. The last identified Use Case 2 (UC2) is defined in this framework to support Broadband services exploiting a non-real time IP connectivity, such as web browsing, file transfer traffic, or on demand audio/video streaming. GEO satellite provides continuous service over time and supports extended sessions without the need for handovers to other satellites or interruptions. Definitively, the presented IAB architecture is suitable to support events where the density of terminals wanting to access the Internet is particularly high, as represented in Fig. 6. Therefore, it may be necessary to deploy an additional network element (i.e., the "Terrestrial IAB-node" in figure) that can dynamically reach the target area and relay part of the transmissions through the IAB network served by a satellite link. SatCom in this scenario allows a dynamic deployment of an IAB network when required while it can always serve a portion of NTN users provided with FWA access in case of lack of terrestrial infrastructure, or as complementary access.

Definitively, the selection of a hybrid approach is considering also the current state of UE terminal technology, a full-satellite approach would limit access to the IAB network to only those terminals supporting SatCom.

## 4. Simulator design and implementation

To validate the possibility of IAB as an enabling technology in the integration between terrestrial and non-terrestrial 5G nodes, a performance evaluation is needed. Specifically, two use cases have been

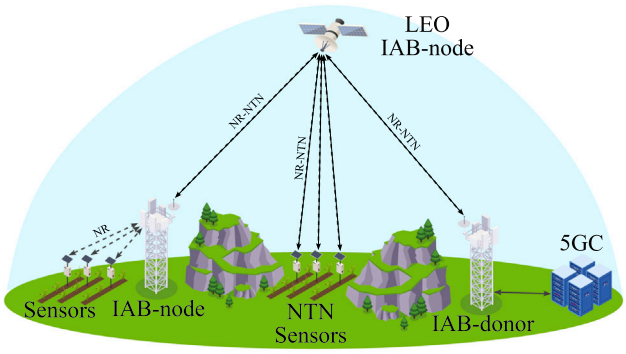


**Fig. 5.** Sensor networks and IoT — UC1.

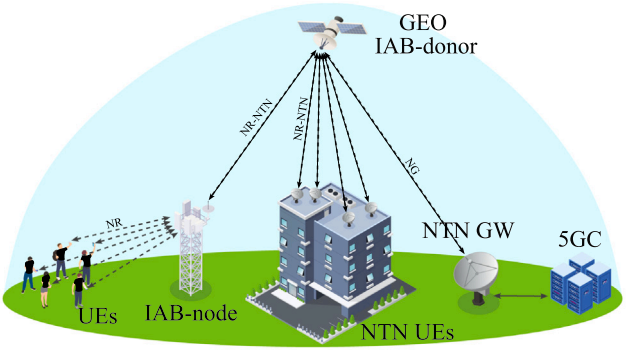


**Fig. 6.** Broadband services — UC2.

defined in Section 3.3, each with a different architecture tailored to support the particular target service (i.e. IoT or broadband applications). The actual applicability of these should be studied in order to validate the design phase, and at the same time identify the limitations and weak characteristics of the particular scenario. However, there is a lack of simulation tools capable of jointly evaluating 5G architectures, IAB features and nodes, as well as satellite radio links and mobility models. To cover this aspect, a platform for system-level assessments described in what follows has been implemented.

The starting point for the development of such a simulator is the open source and C++ based *5G-air-simulator* tool. Similar to other tools for system-level analysis, it consists of a series of C++ objects, or modules, whose methods can be called according to an event-driven logic. Using this paradigm, events (e.g. transmission of a frame and subsequent reception) are scheduled according to the order determined by a simulation calendar [26]. In its native version,[2] the 5G-air-simulator provides the capability to simulate different architectures, functionalities and procedures that comply with the 5G NR standards. In particular, the presence of the following features led to the choice of such a platform:

- **RAN Components**: each simulated scenario is composed by UEs and gNB, both part of the 5G RAN. They are implemented with the base classes `UserEquipment.cpp` and `GNodeB.cpp`, respectively. Different mobility models can be linked to UEs to reproduce deterministic and stochastic user movements (e.g. the *Manhattan Model* to reproduce urban environments).
- **Complete Protocol Stack**: the entire 5G protocol stack is implemented to simulate transmission and reception logic between

[2] The source code of the 5G-air-simulator native version is freely available at: https://telematics.poliba.it/5gairsim-tool/.

network devices. Specifically, each component of the stack has a related C++ class in charge of managing data flows and handover procedures (i.e. RRC), performing header compression (i.e. PDCP), handling buffering, segmentation, reassembly, concatenation and retransmission of data units (i.e. RLC), and implementing data transmission and reception (i.e. MAC). Additionally, different data transfer modes are supported at RLC layer and HARQ and Adaptive Modulation and Coding (AMC) procedures are included in the MAC module. On top of these communication functions, there is a set of applications generating several flows according to typical packet generation models.

- **Link-to-System Channel Model**: to provide a lightweight but accurate wireless channel simulation, it is possible to model the received signals by adopting a set of pre-computed values as a function of the communication nodes characteristics. These values can be computed in a script that accurately emulates the radio channel, or taken from standardization bodies reports. Many models are already available in the simulator to abstract the main physical-layer phenomena, including path loss, shadowing, penetration loss, fast fading, noise power, and interference.

For each simulated scenario, it is necessary to make a dedicated C++ function in which all components of the simulations are initializedA simulation can be launched running the simulator executable from the shell, passing as parameters the name of the scenario and a set of values that are handled by the scenario to configure itself. As output, the tool generates a textual trace reporting information about events happening in the simulation. To extract Key Performance Indicators (KPIs), the console output has to be processed. Examples of KPIs are Average User Throughput, Average Packet Loss Ratio (PLR), Average Random Access Collision Rate, Cell Goodput, Average Packet Delay and Cell-Edge Throughput. Starting from the original implementation of the simulator, several changes, described in deep detail the following sections, have been implemented in order to support the simulation of IAB scenarios integrating satellite nodes.

### 4.1. IAB-node and functions splitting

Natively, the simulator handles communications between UEs and gNB through a set of classes implementing user-plane functions. The different layers are enclosed in the single container class `Protocol-Stack.cpp`, of which all nodes are equipped thanks to a logical link obtained through pointers association (i.e., the node object store the memory index of the protocol stack container object, and vice versa, thus allowing at each time of the simulation to retrieve attribute or use methods of the linked object). To implement the IAB-node, it is assumed that it performs a dual function:it acts (i) as a gNB on the IAB-DU side, and (ii) as a UE on the IAB-MT side. Based on this logic, the class representing the IAB-node device has been developed by extending `GNodeB.cpp` (i.e. wrapper class for gNB) with an instance of `UserEquipment.cpp` (i.e. UE implementation). To avoid delving into source code details, Fig. 7 illustrates a high-level description, together with the reference classes, of such design. Since the native UE and gNB classes have been adopted, the implemented IAB-node is able to communicate with both UEs and gNBs (which also acts as an IAB-donor in the architecture). Transmissions at the physical layer can be simulated by means of (i) one of the terrestrial propagation models already implemented in the simulator, and (ii) the proposed satellite link-to-system model, making this implementation suitable for simulating terrestrial and non-terrestrial architectures. Forwarding operation between IAB-DU and IAB-MT is achieved through a new layer in the respective `protocol-stack.cpp`, namely `relay-sender.cpp` and `relay-receiver.cpp`. The way in which a communication through an IAB-node is simulated may be summarized as follows. The source node (e.g. UE or gNB) generates a packet flow according to the application model adopted, such as Constant BitRate (CBR) (by means of `CBR.cpp`), Voice over IP (VoIP) (by means of `VoIP.cpp`) or File Transfer Protocol (FTP) (by means of `FTP.cpp`). Packets are then processed by each element of the protocol stack until they are received, through the physical layer, at the next IAB-node (i.e. IAB-DU or IAB-MT). Here, they move up the protocol stack until they reach the *RelayReceiver* application, which is responsible of sending packets through the associated *RelaySender* application installed on the other interface of the IAB-node. Finally, packets can be sent to the destination node via the native communication mechanism or delivered to a further IAB-node where the logic will be repeated. Fig. 7 pictorially illustrates this process.

With the aim of preserving a spectrum resources, this work analyses the *In-band* configuration, which requires the use of the same channel for access and backhaul [18]. Such a resource sharing mechanism demands that the IAB-DU and IAB-MT radio interface cannot operate simultaneously unless they have proper frequency or spatial multiplexing capabilities. Due to this half-duplex constraint, the uplink (downlink) channel on the access side cannot operate simultaneously with the uplink (downlink) channel on the backhaul side, requiring the adoption of a TDD solution. At the time of writing, no temporal division patterns between access and backhaul have been standardized by 3GPP yet, therefore, some custom configurations depicted in Fig. 8 have been adopted.

Specifically, the (a), (b) and (c) patterns have been adopted in the UC1 scenario, distributing in different time slots a period for access and a period for backauling. On the other hand, (d) has been used for analyzing UC2, with an equal amount of time slot for access and backhaul, with the backhaul period exploited for simultaneous uplink and downlink transmission through the FDD approach. It is worth noting that, despite the possibility in NR technology to allocate time resources of the order of a single symbol [27], each block corresponds to an entire timeslot of 1 ms (i.e. 14 symbols), that is the slot duration for Sub Carrier Spacing (SCS) of 15 kHz. Moreover, whenever it is necessary to switch from a downlink to an uplink phase, one slot is left idle as a guard time for signal propagation purposes. It is not necessary instead, when switching from uplink to downlink since these two phases are always synchronized thanks to the TA functionality.

### 4.2. Satellite channel and movement

The system-level simulation phase has been preceded by a study dedicated to the ground-to-satellite link. Its scope is twofold: to enable testing and evaluation of different configurations for physical interface of terrestrial and satellite nodes, and to compute a set of values that, given as input to the simulator, allow reproducing the ground-to-satellite radio channel via *Link-to-System* feature (as described in Section 4). Reference Signal to Noise Ratio (SNR) and Link Budget (LB) values are already present in 3GPP standards [6], nevertheless the implementation of a system level simulator that accurately accounts for the impact of a satellite node in the IAB architecture requires a detailed channel characterization for different elevation angles, especially in LEO scenarios. Note that, this aspect is actually not covered in the current versions of the standards.

By analyzing the use cases chosen to evaluate the proposed IAB architectures, it can be noted that the satellite link is established between different types of entities. Specifically, UC1 considers a LEO-type satellite that establishes a radio link with reduced capabilities devices (i.e., NTN Sensors) or terminals comparable to base stations (i.e., IAB-nodes). Similarly, UC2 envisages a GEO satellite communicating directly with a fixed node (i.e., NTN UE), or establishing a link with a base station (i.e., IAB-node). Therefore, different configurations have been considered for the satellite and the terrestrial node. Regarding the ground platform, the adopted configuration setups are summarized in Table 2, where *Handheld* represents a simple node configuration with limited capabilities in terms of antenna directivity and trasmission power (as in the case of NTN sensors), while IAB-nodes or fixed NTN

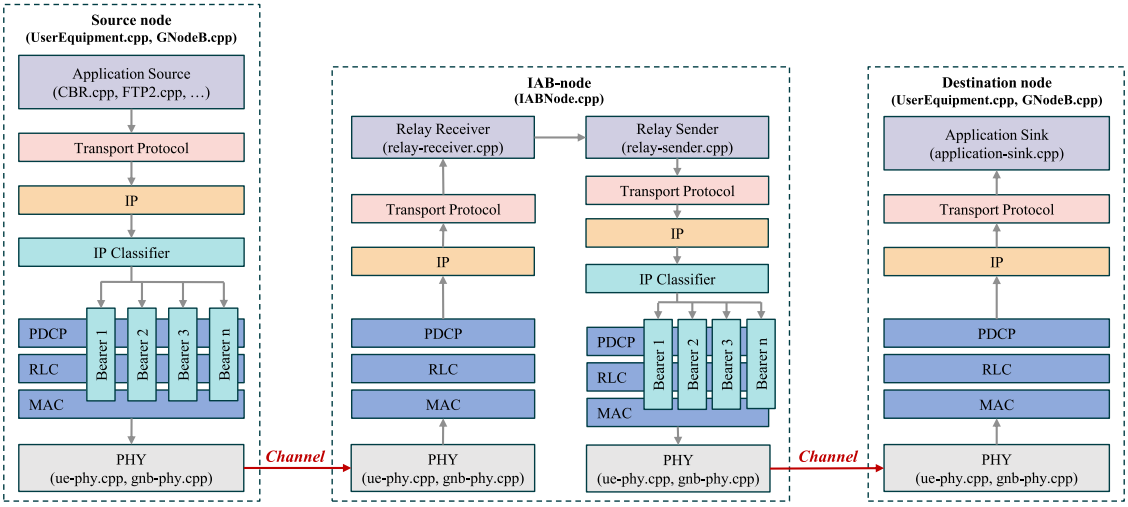


**Fig. 7.** High level description of IAB-node relay function implementation.

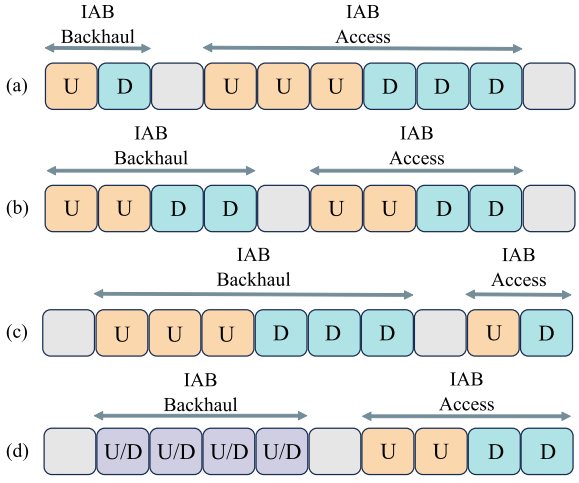


**Fig. 8.** Adopted TDD patterns to separate access and backhaul periods.

UEs are modeled through terminals named *VSAT*. It is noteworthy that the configuration adopted for*VSAT* to GEO employs a transmission Equivalent Isotropically Radiated Power (EIRP) value expressed as power density, as suggested in [6]. On the other hand, for a VSAT communicating with a LEO-type satellite, any configuration is provided in 3GPP technical documents, thus a fixed transmitting power value has been set accordingly. Four configurations have instead been considered for what concerns the satellite side, whose related parameters are provided in Table 3. $SAT_A$ and $SAT_B$ are employed in LEO-type platform, with the former being a suitable configuration for small size satellites and the latter being described in [6], which also provides the parameters adopted in $SAT_C$ and $SAT_D$, two reference configuration for VSAT to GEO access in FR1. It is also worth noting that the transmission power density for the satellite node is in accordance to what defined in [28], which does not specify any upper limit for the power radiated by a Wide-Area Base Station (BS).

Each radio interface configuration has been set up according to three different case studies:

- *Case study 1*: the link is established between a terrestrial *Handheld* and a satellite configured as $SAT_A$ or $SAT_B$;
- *Case study 2*: a *VSAT* communicates with a satellite configured as $SAT_A$ or $SAT_B$.

**Table 2**
Parameter setting for terrestrial nodes.

| Configuration name | *Handheld* | *VSAT* | *VSAT* |
|---|---|---|---|
| Target satellite platform | LEO | LEO | GEO |
| Antenna type | Isotropic antenna element | Parabolic dish reflector | Parabolic dish reflector |
| Circular reflector diameter | / | 1 m | 1 m |
| Circular reflector efficiency | / | 0.6 | 0.6 |
| Antenna Tx max gain | 0 dBi | 30 dBi | 30 dBi |
| Tx EIRP | 23 dBm | 38 dBm | 34 dBW/MHz |

**Table 3**
Parameter setting for satellite nodes.

| Configuration name | $SAT_A$ | $SAT_B$ | $SAT_C$ | $SAT_D$ |
|---|---|---|---|---|
| Orbit | LEO | LEO | GEO | GEO |
| Altitude | 600 km | 600 km | 35 786 km | 35 786 km |
| Antenna type | Circular patch antenna | Parabolic dish reflector | Parabolic dish reflector | Parabolic dish reflector |
| Circular reflector diameter | / | 2 m | 12 m | 22 m |
| Circular reflector efficiency | / | 0.6 | 0.6 | 0.6 |
| Antenna Tx max gain | 6 dBi | 30 dBi | 45.5 dBi | 51 dBi |
| Tx EIRP | 34 dBW/MHz | 34 dBW/MHz | 53.5 dBW/MHz | 59 dBW/MHz |

- *Case study 3*: the *VSAT* accesses to a GEO satellite. The on-board configuration can be $SAT_C$ or $SAT_D$.

The evaluation is performed in both uplink and downlink directions, adopting the methodology described in [29] and the channel model proposed in [19] to realize a MATLAB Script computing satellite link performance. The main parameters used for the link level analysis are summarized in Table 4. The implemented MATLAB script computes the LB according to (1), where $P$ is the node transmitting power, $FSPL(\theta_{el})$ is the Free Space Path Loss (FSPL), $G_{Ant}$ includes the receiver and transmitter antenna gains, $DCF_{Ant}$ reshapes the latter according to a Diagram Correction Factors (DCFs) and $L_{imp}(\theta_{el})$ comprises the others impairment effects due to air, atmospheric conditions, scintillation and polarization attenuation phenomena.

It can be noted that, from the system-level simulator point of view, it is necessary to derive the value of SNR, or Signal to Interference plus Nois Ratio (SINR) in the case of multiple nodes transmitting on

**Table 4**
Parameter setting for link level analysis.

| | | | |
|---|---|---|---|
| Carrier frequency | 2 [GHz] | Resource block structure | 12 x SCS with SCS = 15 [kHz] |
| Bandwidth configurations | {1, 25, 52, 79, 106} RB | Elevation angle range | 5 : 90 [°] |
| Satellite, terrestrial node noise figure | 5, 7 [dB] | Elevation steps | 0.1 [°] |
| Satellite, terrestrial node antenna temp. | 150, 290 [dB] | Ambient temperature | 290 [K] |
| LEO satellite altitude | 600 [km] | GEO satellite altitude | 35786 [km] |

the same band, for each Resource Block (RB). This is accomplished by first dividing the LB by the number of RBs, and then subtracting from each of them the receiver sensitivity value computed in (2). Here, $BW$ represents the RB bandwidth, $NF$ the Noise Figure of the receiving node, $k_B$ the Boltzmann constant, $T_{ant}$ the receiving antenna noise temperature and $T_{ant}$ the ambient noise temperature.

$$LB\left(\theta_{el}\right) = P|_{\text{dBm}} + G_{Ant} + DCF_{Ant} - FSPL\left(\theta_{el}\right) - L_{imp}\left(\theta_{el}\right) \tag{1}$$

$$RS|_{\text{dBm}} = 30 + 10 * log10(k_B * BW) + NF + + 10 * log10\left(\frac{T_{amb} + (T_{ant} - T_{amb})}{10^{0.1*NF}}\right) \tag{2}$$

Regarding the different radiation patterns, a circular patch antenna (i.e., $SAT_A$) is modeled according to the DCF in (3):

$$DCF_{Ant,Circ} = 4\,\frac{\cos^2\left(\varphi\left(J_0(\beta) - J_2(\beta)\right)^2\right) + \cos^2(\alpha)\sin^2\left(\varphi\left(J_0(\beta) + J_2(\beta)\right)^2\right)}{\int_0^{\frac{\pi}{2}}\left(\left(J_0(\beta) - J_2(\beta)\right)^2 + \cos^2\left(\theta\left(J_0(\beta) + J_2(\beta)\right)^2\right)\right) sin\theta d\theta} \tag{3}$$

For the sake of readability, $\zeta\varrho\sin\alpha = \beta$ has been posed, where $\zeta$ is the free space phase constant and $\varrho$ is the effective radius of the circular patch. Furthermore, $\alpha$ is the inclination angle, $\varphi$ is the azimuth angle and $J_n$ is the Bessel function of the first kind [30]. The parabolic dish reflectors (i.e., $SAT_B$, $SAT_C$, $SAT_D$ and $VSAT$) are modeled according to (4)

$$DCF_{Ant,Refl} = 4\left|\frac{J_1\ (2\pi\,(f/c)\,(d/2)\,sin\alpha)}{(2\pi\,(f/c)\,(d/2)\,sin\alpha)}\right|^2 \tag{4}$$

with $f$ being the carrier frequency, $d$ the dish diameter, $\alpha$ the inclination angle and $J_n$ the Bessel functions of the first kind [19].

Results obtained in terms of LB are depicted in Figs. 9–12. In particular, Fig. 9 shows the downlink and uplink channel behavior for *Case Study 1*, as a function of the elevation angle. As expected, a higher transmission power from the satellite to the ground user generally results in a higher LB for the downlink if compared to the uplink. The difference between the two antennas is also evident, with $SAT_A$ allowing higher receiving power for small angles with respect to $SAT_B$. This trend inverts starting from ~85°, with the peak value reached at 90°

Fig. 10 illustrates the results achieved for *Case Study 2*. Compared with the *Handheld* node, a VSAT can also perform pointing, keeping the satellite centered in the main lobe of the antenna [31]. For sake of completeness, this last feature has also been evaluated, naming it as *Track*. The LB for the different proposed configurations is shown in Fig. 10 for the downlink, and in Fig. 11 for the uplink. It can be observed that, when pointing is not performed, the way the LB changes as the elevation angle varies is strongly affected by the radiation pattern of both antennas. Satellite tracking, on the other hand, results in a curve behavior influenced by the radiation pattern of the on-board satellite

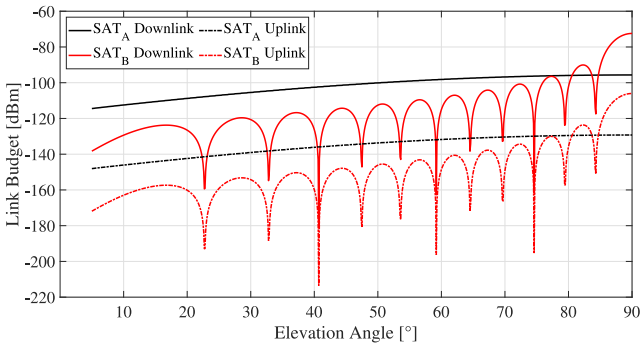


**Fig. 9.** Downlink and uplink LB for *Case Study 1* as a function of the satellite elevation angle.

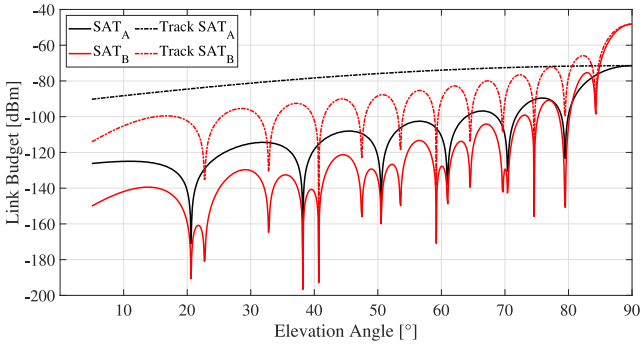


**Fig. 10.** Downlink LB for *Case Study 2* as a function of the satellite elevation angle.

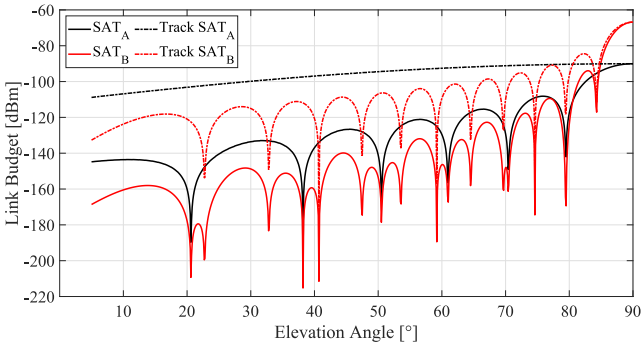


**Fig. 11.** Uplink LB for *Case Study 2* as a function of the satellite elevation angle.

antenna, but with higher receiving power values due to the maximized gain of the earth node.

Finally, Fig. 12 shows the LB for *Case Study 3* in downlink and uplink directions. It is worth noting that the aforementioned pointing is considered always adopted in the case of GEO satellites, being their position fixed in terms of geocentric coordinates. Here again, it can be seen that the pattern of the parabolic antenna creates zones where the LB is severely low.

To complete the characterization of the satellite channel it is also necessary to model the decoding process of the transmitted frames. To this end, the MATLAB 5G Toolbox has been exploited to compute the BLock Error Rate (BLER) curves for each configuration of Modulation and Coding Scheme (MCS), as a function of the SNR. Regarding the MCS, it should be noted that since there are three tables of MCS configurations, the most flexible Table 5.1.3.1-1 defined in [32] has been considered. Each BLER percentage has been computed by simulating the forwarding of 100 blocks over the complete 5G transmission/reception chain that considers the steps that follow. First,

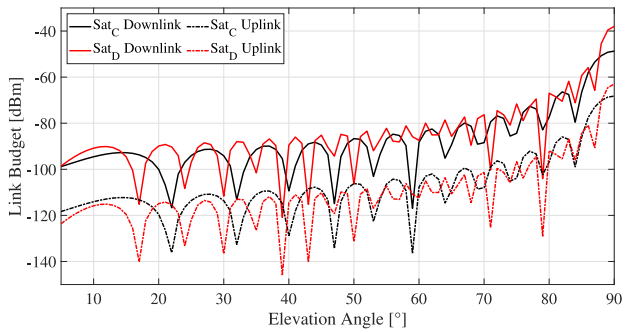


**Fig. 12.** Downlink and uplink LB for *Case Study 3* as a function of the satellite elevation angle.

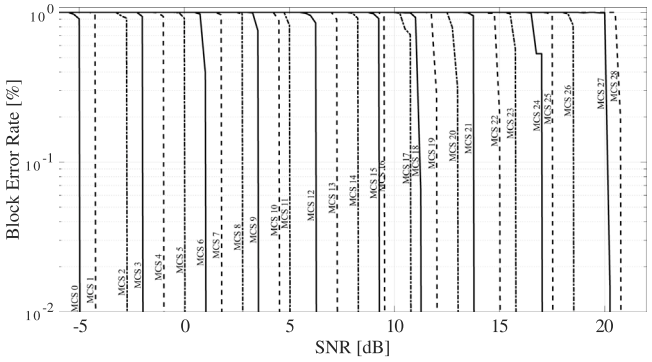


**Fig. 13.** Block error rate as a function of the SNR, for different MCS indexes.

a random set of symbols are generated and placed in the resource grid to be Orthogonal Frequency Division Multiplexing (OFDM)-modulated. The resulting signal is sent into the propagation channel, adding noise. At receiving side, a time synchronization is applied, and the offset associated with the strongest multipath component across all the channel is determined and then compensated. The synchronized signal is then OFDM-demodulated, taking into account the channel effects for each Resource Element (RE). The distortion introduced by the channel is compensated and the equalized symbols are decoded to obtain the bit sequences, checking for errors. Finally, if the Transport Block (TB) is considered as not successfully decoded the block is marked as erroneous. The results of the study are depicted in Fig. 13.

As seen in the link-level study phase, the main input parameter for defining the SNR in a satellite communication is the elevation angle. Since both LEO and GEO satellites are used in the reference use cases, two dedicated mobility models have been developed. A mobility model can be associated with a node (i.e., UE, gNB, IAB-node) to keep track of its location during the temporal evolution of the simulation. For LEO satellites, a trajectory is modeled hovering above the earth node (or the cell of interest) at a speed of 7059.22 m/s. For GEO satellites, on the other hand, even though mobility is not required, a dedicated model has been implemented. It simply computes the slant range as a function of the elevation angle, thus defining the satellite position. Regarding the Link-to-System model, it has a crucial importance, since it provides a simplified yet accurate representation of transmission, propagation, and reception functionalities. It combines link-level analysis, carefully carried out in a dedicated environment, with a system-level simulation tool. The simplified channel model includes SNR expressions for both downlink and uplink channels, along with BLER curves for each transmission mode. The parameters in terms of link budgets, SNR, and BLER, with associated input values (e.g., $x$-axis represented by angle or SNR) have been imported into the simulator in the form of matrices, effectively representing the *SNR curves* and *BLER curves*

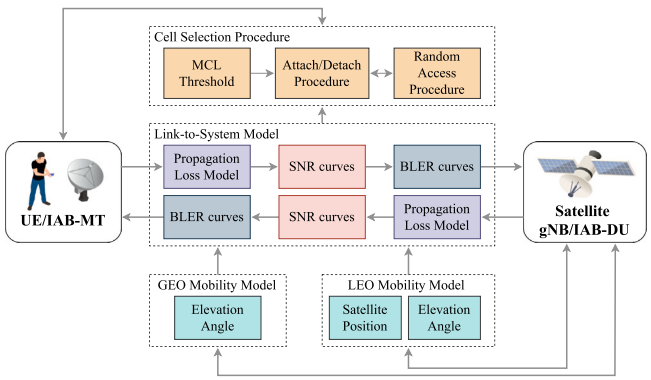


**Fig. 14.** Overall description of the Link-to-System model handling ground-to-satellite communications.

blocks in Fig. 14. In this figure the implemented adaption module is summarized, highlighting how the different blocks interoperate. When a ground node (UE or IAB-node), needs to transmit to a satellite node (gNB or IAB-donor), and vice versa, the transmitted signal is modeled through a Power Spectrum Density (PSD) for each assigned RB, and passed to the Link-to-System Model. It, in turn, establishes how much the signal decays during propagation by extrapolating the final SNR value from the curves computed in MATLAB. In the case of bounded transmission power, the received signal power, and thus the SNR, is spread over all radio resources. To retrieve a single effective SNR, a Mutual Information Effective SNR Mapping (MIESM) method is adopted. This information is used on the one hand to estimate the BLER for the received data block, and, on the other hand, to drive the link adaptation procedure. The Channel Quality Indicator (CQI) feedback is communicated to the other node and used by the AMC module. The latter seeks the most suitable MCS for upcoming transmissions. Moreover, during resource allocation, the MCS is employed to calculate the Transport Block Size (TBS) through a standardized procedure. Regarding mobility models, these instantly provide information on the position of the satellite, and thus on the elevation angle to be used to choose the most suitable SNR. Finally, the channel information offered by the Link-to-System Model makes it possible to decide when the attachment to the gNB is possible or not.

### 4.3. Implemented reference scenarios

Aiming to derive simulation results and evaluate the performance of satellite IAB architectures, reference scenarios have been implemented, each of which simulates a section of the considered use cases. If not otherwise specified, the parameters used in all scenarios are those listed in Table 5. The two use cases and different parts of the simulated architecture result in 8 different scenarios, described in what follows. For what concerns UC1, a scenario focuses on the part of the architecture depicted in Fig. 15(a). Here the sensors directly access the satellite IAB-node, which in turn will forward data to the terrestrial donor. Performance can be evaluated employing an application that sends packets from the UE to the IAB-donor (i.e., uplink), and vice versa (i.e., downlink), through the `UC1DirectUl` and `UC1DirectDL` simulation scripts, respectively. The second scenario focuses on the part of the architecture shown in Fig. 15(b), with the sensors accessing the network through a terrestrial IAB-node, which is responsible for forwarding the data to the satellite IAB-node, which in turn will forward it to the terrestrial donor. Also here the architecture can be simulated in uplink and downlink directions through the `UC1RelayUl` and `UC1RelayDl` scenario definition scripts, respectively. With respect to the UC1 simulations, the main parameters that can be tuned are the number of satellites per orbit, the number of users, the configurations for the satellite on-board antenna, the TDD pattern between backhaul

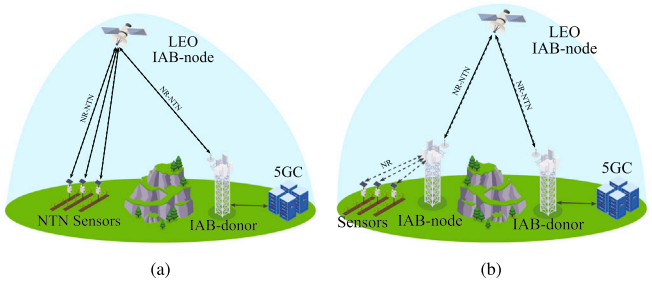


**Fig. 15.** Part of the architecture modeled by the scenarios `UC1DirectUl`, `UC1DirectDl`, `UC1RelayUl` and `UC1RelayDl`.

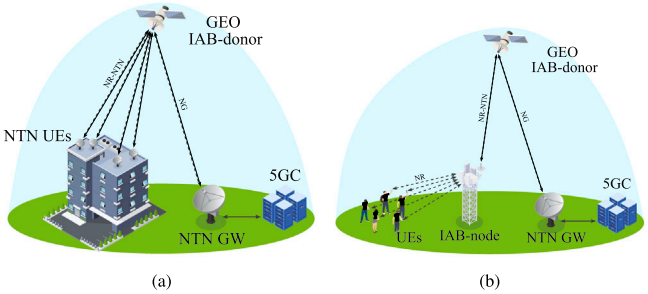


**Fig. 16.** Part of the architecture modeled by the scenarios `UC2DirectUl`, `UC2DirectDl`, `UC2RelayUl` and `UC2RelayDl`.

**Table 5**
Default simulation setting for use case 1 and use case 2 reference scenarios.

| | Use case 1 | Use case 2 |
|---|---|---|
| Bandwidth | 20 [MHz] | 20 [MHz] for TDD, 10 Ul/10 Dl [MHz] for FDD |
| TDD pattern | TDD (a), TDD (b), TDD (c) | TDD (c) |
| Cell radius | 1 [km] | 1 [km] |
| gNB/IAB-node position | (0, 0) [m] | (0, 0) [m] |
| UE position | (100, 100) [m] | (100, 100) [m] |
| Duration | 294.5 [s] | 20.0 [s] |
| Satellite mobility | From 30°, to 90° and back to 30° | Fixed configurable elevation angle |
| Application flow | IoT-like traffic of 400 bps via CBR application generating 250 B every 5 s | Media streaming traffic of 8 Mbps via CBR application generating 5000 B every 5 ms |

and access, and the configuration of the used application (CBR, by default).

Regarding UC2 instead, two scenarios have been implemented, simulating different parts of the architecture. In Fig. 16(a) a fixed station directly accesses the satellite gNB. No IAB-nodes are used here, while to offload data to the ground a dedicated link (whose performance is out of scope of the study) is provided. To evaluate performance, an application is simulated at the satellite side, sending data to the ground station (i.e., downlink) or vice versa (i.e., uplink), through the `UC2DirectUl` and `UC2DirectDl` simulation scripts, respectively. In Fig. 16(b) terrestrial UEs access the network through a terrestrial IAB-node, responsible for relaying data to the IAB-donor on the GEO satellite. Uplink and downlink traffic simulation are performed through the `UC2RelayUl` or `UC2RelayDl` configuration scripts. The main parameters that can be tuned in UC2 simulation are the number of users, the elevation angle, the configurations for the satellite on-board antenna, and the configuration of the used application (CBR, by default).

## 5. Simulation results

The following section aims to evaluate the performance of the use cases identified in Section 3.3 using the simulation tool whose implementation is described in Section 4. Despite the simulator ability to vary several parameters, the following test results have been carried out using a single satellite per constellation (i.e. LEO scenario), a single radio resource grid configuration (i.e. 20 MHz bandwidth and 15 kHz sub-carrier spacing) and only considering the uplink direction, which is the most critical aspect of the architecture. The single satellite constellation allows a more manageable and comprehensible analysis of the system performance, without adding the complexity of constellations or clusters, for which the RACH procedures require a much more complex simulator implementation. Similarly, using a fixed bandwidth and SCS permits a linear and effective analysis of specific aspects of the architecture. The simulation results are divided into three parts, investigating (i) the registration time needed by access users for the two use cases, (ii) the time to deliver packets and the measured throughput for access and backhaul of UC1 and (iii) the time to complete transmission and measured throughput for access and backhaul of UC2.

### 5.1. Scenario #1

Before assessing the capabilities of the identified architectures in terms of the services that can be offered, it is important to analyze whether one or more users are able to access simultaneously the network, and with what impact on the system performance. In particular, experimental tests conducted on a local 5G System (5GS) installation made it possible to model the traffic, in terms of packets exchanged, between the user and the core network during initial procedures, which include access to the radio channel, network registration, and Protocol Data Unit (PDU) session establishment. For the scope, the *free5GC* [33] is used to implement a 5GC, and *UERANSIM* [34] is used to emulate UE devices in a NG-RAN. Tests were conducted in a local virtual environment. Such traffic flow has been modeled and used in `UC1RelayUl` and `UC2RelayUl` scenarios. Several simulations have been performed, in which per-user end-to-end time required to complete packets transmission has been measured. The number of users in the cell has been set to {1, 5, 20, 50}, thus evaluating the impact of multiple UEs on the access time of a single device. Fig. 17 refers to the results obtained for UC1 when TDD(a), TDD (b) and TDD (c) patterns are used, respectively (please refer to Fig. 8). For each TDD pattern, different antenna configurations have been also evaluated, i.e. $SAT_A$, $SAT_B$, with and without tracking the satellite position (only for terrestrial IAB-node). In general, there is an evident impact of the number of users attempting to register, on the registration time of the single UE. This is mainly due to the bottleneck in the backhauling link in charge to forward the flow of multiple users accessing the network at the same time. Moreover, the duration of the initialization phase is affected by collision events during the RACH procedure. For what concern antenna configurations, it is noteworthy that the tracking system has a considerable positive impact on system performance. In fact, focusing on the curve for TDD (a), using "Track $SAT_A$" a single user completes the registration in 764 ms, while this time rises to 9476 ms in case of 50 users. For "Track $SAT_B$" instead, much higher values are experimented, of 33 S for 1 user to 99.5 s for 50 users, with an absolute maximum of 137.84 s for 50 users and "$SAT_A$". Such high times can be attributed to the link closure which, especially when pointing is not employed, occurs for great elevation angles (note that the satellite reaches 90° of elevation about half the simulation time, which is of about 147 s). Visually, the different configurations of TDD do not highlight marked differences. For example, taking the 20-user point of the "$SAT_A$" curve as a reference, it can be noted that

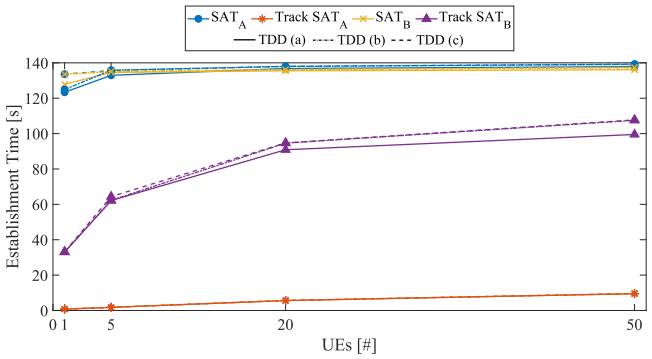


**Fig. 17.** Registration time in UC1 through relay access for different user numbers, antenna configurations and TDD patterns.

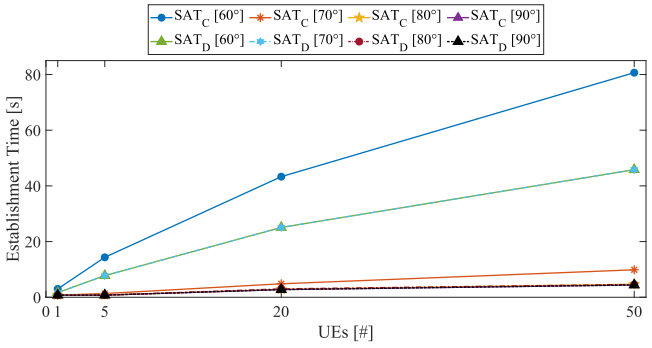


**Fig. 18.** Registration time in UC2 through relay access for different user numbers, elevation angles and antenna configurations.

it equals 136.78 s for TDD (a), 137.98 s for TDD (b) and 138.024 s for TDD (c). This slight increase, observable for almost all the points in the graph, can be attributed to a lower time dedicated to the access link.

Fig. 18, on the other hand, shows the results of UC2 with $SAT_C$ and $SAT_D$ respectively. Here each curve represents the registration time of the single UE for 60°, 70°, 80° and 90°. In general, this time increases with the number of users, reaching high values (i.e., more than 10 s) due to poor channel quality with 60° and 70° for $SAT_D$, 60° for $SAT_C$. In fact, as observable in the satellite link modeling of Section 4.2, a parabolic antenna onboard a GEO satellite cannot uniformly cover a large area, leaving users having the satellite at low elevation angles (i.e., under ∼50°) uncovered.

### 5.2. Scenario #2

Focusing on UC1, in this section some performance metrics, i.e., end-to-end time required to deliver packets, forwarding time of the IAB-node, and measured application throughput on each wireless link (access and backhaul), are evaluated. To derive these simulation results, `UC1DirectUl` and `UC1RelayUl` scenarios have been considered, in which a single user generates IoT-like traffic of 400 bps directed to a virtual server located on the IAB-donor. Fig. 19 shows the average end-to-end data transmission time and access link capacity respectively for both scenarios with different antenna configurations and TDD patterns. Note that, for `UC1DirectUl` only "$SAT_B$" has been evaluated (labeled as "Direct $SAT_B$"). Indeed, "$SAT_A$" configuration does not allow for any elevation angle to achieve the minimum SNR needed to close the link. As also observed in the previous test case, the adopted antenna configuration has a strong impact on the overall performance. Specifically, the "Track $SAT_A$" configuration allows the link to be closed from very small elevation angles, thus permitting an

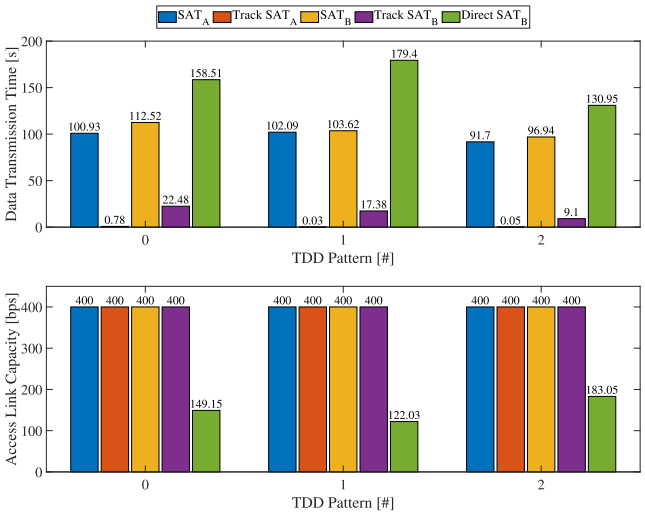


**Fig. 19.** Access application throughput and end-to-end data transmission time in UC1 through relay or direct access, for different antenna configurations and TDD patterns. (For interpretation of the references to color in this figure legend, the reader is referred to the web version of this article.)

end-to-end delay of 780 ms for TDD (a), 55 ms for TDD (b) and 29 ms for TDD (c). On the other hand, concerning the other configurations, the delay drastically increases with a minimum of 9.1 s for TDD (c) and "Track $SAT_A$", and a maximum of 112.52 s for TDD (a) and "$SAT_B$". Also in this case, it is possible to state that delays are affected by the quality of the channel, that does not reach the minimum transmission requirements for low elevation angles. The minimum angle at which the link can be closed depends on the configuration, and as the link budget is not linear (see Section 4.2), it may not be available again after a few seconds from the moment the node starts transmitting. This also holds for the "Direct $SAT_B$" case where delays are even more pronounced. Moreover, results show minor differences among the different TDD patterns, with lower delays experimented for TDD (c). Finally, access throughput results are coherent with the packet generation rate for the `UC1RelayUl` case, being the terrestrial link oversized for the traffic, while it struggles to deliver data with the same generation rate in the `UC1DirectUl` case. Here again the problem can be attributed to the satellite link not being closed for lower elevation angles.

Regarding the measured link capacity and forwarding time at the backhaul side, the analysis focuses on `UC1RelayUl` only. It is worth noting that this scenario presents two backhaul links (as depicted in Fig. 15(b)). The first is established between the terrestrial IAB-node interfacing ground users in the access, with the satellite IAB-node data are forwarded to. The second is established between the satellite IAB-node and the terrestrial IAB-donor data are offloaded to. Results shown in Fig. 20 concern the first backhaul link, while results in Fig. 21 are related to the second one. The behavior with different antenna configurations is very similar between the two links; this is due to the use of the same channel model and parameter setting used for the simulation of the link (i.e. VSAT to $SAT_A SAT_B$ for the first, $SAT_A SAT_B$ to VSAT for the second). Also the forwarding delay on backhaul links results to be very small for "Track $SAT_A$" configuration, giving also the possibility to reach an application rate equivalent to the packet generation flow for this IoT-like specific case. The other configurations, on the other hand, take several seconds to forward the data, thus experimenting a lower rate. The reason for this is again that, due to the antennas directivity, it is only possible to transmit only from a satellite position on. Finally, comparing the values obtained on the two links, it is possible to note a slightly lower performance for the second, due to the delay already collected by the first.

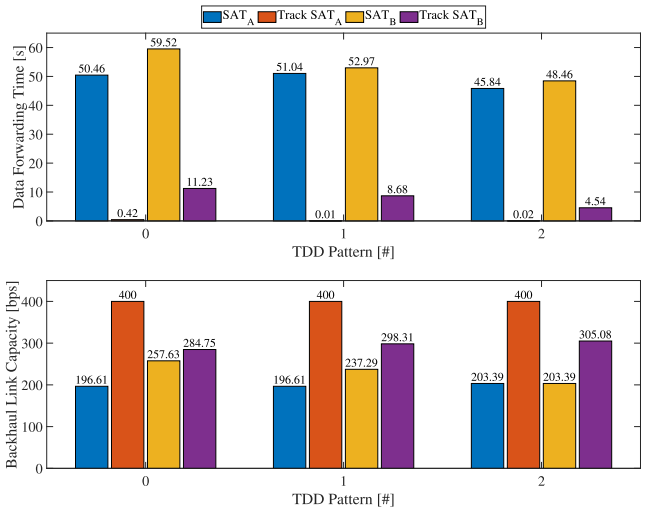


**Fig. 20.** Application throughput and forwarding time on the first backhaul link of UC1 through relay access, for different antenna configurations and TDD patterns. (For interpretation of the references to color in this figure legend, the reader is referred to the web version of this article.)

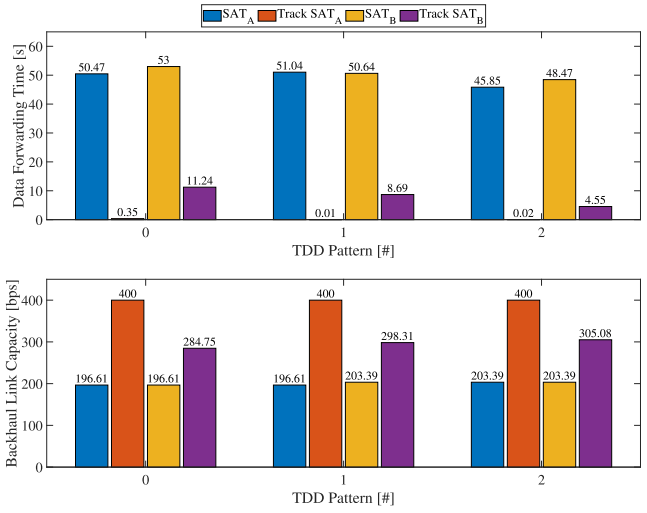


**Fig. 21.** Application throughput and forwarding time on the second backhaul link of UC1 through relay access, for different antenna configurations and TDD patterns. (For interpretation of the references to color in this figure legend, the reader is referred to the web version of this article.)

### 5.3. Scenario #3

For the latest scenario, a set of `UC2DirectUl` and `UC2RelayUl` simulations have been performed with the GEO satellite placed at different elevation angles (for the sake of clarity, it is simulated a GEO satellite perpendicular to the equator, and a user at a parallel) to derive the end-to-end data transmission time, the forwarding time and the application throughput on the single link. The packet flow simulates an application generating a media streaming traffic of 8 Mbps, during a 10 s simulation. The end-to-end delay of 10 s and an access throughput of 0 Mbps is observed for all that elevation angles bringing to a poor channel quality of the satellite link. In Fig. 22 results are shown in terms of average end-to-end data transmission time for `UC2DirectUl` and `UC2RelayUl`, and forwarding time on the backhaul link for `UC2RelayUl`. Fig. 23 illustrates application access and backhaul link capacity for `UC2RelayUl`, and only access throughput for `UC2DirectUl`. The analysis is carried out for different elevation angles, with a step of 10°, and both usable antenna configurations

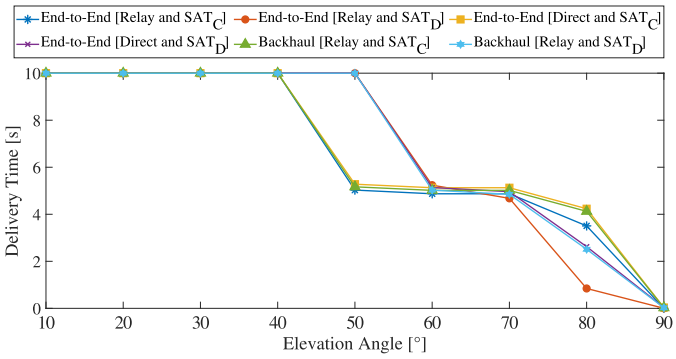


**Fig. 22.** End-to-end delay and forwarding time for access and backhaul links of UC2 through relay or direct access, for different antenna configurations and elevation angles.

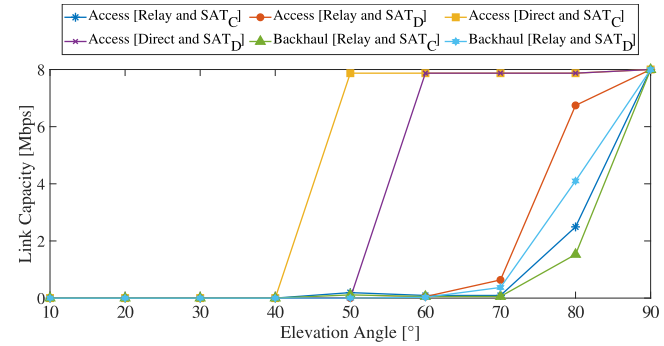


**Fig. 23.** Application throughput on access and backhaul links of UC2 through relay or direct access, for different antenna configurations and elevation angles.

(i.e. $SAT_C$ and $SAT_D$). For both configurations, when data transmission is allowed, the end-to-end delay is around 5 s, with a rate of a few hundreds kb for an angle of up to 70°. These values raise starting from 80°, to reach highest performance for 90° where access throughput saturates at 8 Mbps and delay drops to 3 ms. It can be noted that the end-to-end delay is not strongly affected by the terrestrial node forwarding data to satellite, since similar values are obtained for the direct access (i.e. purple and yellow curve of Fig. 22). The access throughput turns out to saturate at 8 Mbps as soon as communication occurs. This is plausible, since the terrestrial link has been appropriately sized to fully support the data throughput. Also in the backhaul link, for both $SAT_C$ and $SAT_D$ the forwarding delay is around 5 s with a rate of a few hundreds kb for an angle of up to 70°. These values raise at 80° to reach the highest performance at 90°, where backhaul throughput saturates at 8 Mbps and delay drops to 4 ms.

## 6. Conclusions

The study carried out in this paper has resulted in a comprehensive investigation of integrated terrestrial and non-terrestrial mobile architectures, with a particular focus on the employment of satellite IAB-node and satellite IAB-donor. Two use cases have been proposed, UC1 and UC2, designed to support different services. To analyze their performance, a system-level simulator has been developed, carefully taking into account several implementation aspects such as the modeling and subsequent adaptation of the satellite Link-to-System Model, the integration of satellite mobility characteristics, the realization of the IAB-node device, the definition of resource sharing techniques, and the description of basic scenarios adopted to derive simulation results. Results show that, for LEO satellite scenario, the satellite platform significantly influences the time required to complete a transmission because of the intermittent coverage. Conversely, in the GEO satellite

scenario, it is evident that the satellite backhaul link could become a bottleneck in the system, particularly at lower elevation angles. Results also show that the integration NTN with IAB technology is feasible, even if it is strongly influenced by the configuration of the satellite system or, in some instances, the TDD scheme, more than the IAB technology by itself. Future research efforts on this topic could explore (i) the assessment of the impact of handover procedures between multiple satellites of a LEO constellation on overall performance, (ii) adoption of routing logics between IAB-nodes via the BAP protocol, to search for the best route between terrestrial and satellite IAB-nodes (i.e., ISL communications), (iii) implementation of integrated IAB-NTN architectures using Open RAN (O-RAN) softwares, with focus on the satellite link only, (iv) employment of FR2 operating bands, and in particular the range referred to as mmWave.

## CRediT authorship contribution statement

**Daniele Pugliese:** Writing – original draft, Conceptualization, Methodology, Software, Visualization. **Mattia Quadrini:** Writing – original draft, Conceptualization, Formal analysis, Investigation, Methodology. **Domenico Striccoli:** Writing – original draft, Conceptualization, Methodology, Validation. **Cesare Roseti:** Writing – original draft, Conceptualization, Methodology, Validation. **Francesco Zampognaro:** Conceptualization, Methodology, Supervision, Writing – review & editing. **Giuseppe Piro:** Conceptualization, Methodology, Supervision, Writing – review & editing. **Luigi Alfredo Grieco:** Conceptualization, Methodology, Supervision. **Gennaro Boggia:** Conceptualization, Methodology, Supervision.

## Declaration of competing interest

The authors declare that they have no known competing financial interests or personal relationships that could have appeared to influence the work reported in this paper.

## Data availability

No data was used for the research described in the article.

## Acknowledgments

This work was supported by the European Union under the Italian National Recovery and Resilience Plan (NRRP) of NextGenerationEU, in the context of partnership on “Telecommunications of the Future” (PE00000001 - program “RESTART”, CUP: D93C22000910001), national center on “Sustainable Mobility” (CN00000023 - program “MOST”, CUP: D93C22000410001), and partnership on “Cybersecurity” (PE00000007 - program “SERICS”, CUP: D33C22001300002, project ISP5G+). It was also supported by the PRIN 2022 projects INSPIRE (grant no. 2022BEXMXN_01) and HORUS (grant no. 2022P44KA8) funded by the Italian MUR, by the HORIZON MSCA project BRIDGITISE (grant no. 101119554) and the HORIZON JU SNS project 6G-GOALS (grant no. 101139232), and by “The house of emerging technologies of Matera (CTEMT)” project funded by the Italian MIMIT. The results presented in this paper are also part of the outcomes of the SATIABLE project, ESA Contract No. 4000139666/22/UK/AL. Responsibility of the content resides with the authors.

## References

[1] A. Guidotti, A. Vanelli-Coralli, V. Schena, N. Chuberre, M. El Jaafari, J. Puttonen, S. Cioni, The path to 5G-advanced and 6G non-terrestrial network systems, in: 2022 11th Advanced Satellite Multimedia Systems Conference and the 17th Signal Processing for Space Communications Workshop (ASMS/SPSC), 2022, pp. 1–8, http://dx.doi.org/10.1109/ASMS/SPSC55670.2022.9914764.

[2] S. Sirotkin, 5G Radio Access Network Architecture: The Dark Side of 5G, Wiley, 2021, http://dx.doi.org/10.1002/9781119550921.

[3] 3rd Generation Partnership Project, NR; NR and NG-RAN Overall Description; Stage 2 (Release 17), TS 38.300, 2023, (Online Accessed 14 March 2024).

[4] H. Ronkainen, J. Edstam, A. Ericsson, C. Östberg, Integrated access and backhaul a new type of wireless backhaul in 5G, Ericsson Tech. Rev. 2020 (7) (2020) 2–11.

[5] C.-X. Wang, X. You, X. Gao, X. Zhu, Z. Li, C. Zhang, H. Wang, Y. Huang, Y. Chen, H. Haas, J.S. Thompson, E.G. Larsson, M.D. Renzo, W. Tong, P. Zhu, X. Shen, H.V. Poor, L. Hanzo, On the road to 6G: Visions, requirements, key technologies, and testbeds, IEEE Commun. Surv. Tutor. 25 (2) (2023) 905–974, http://dx.doi.org/10.1109/COMST.2023.3249835.

[6] 3rd Generation Partnership Project, Solutions For NR to Support Non-Terrestrial Networks (NTN), TR 38.821, 2023, (Online Accessed 14 March 2024).

[7] V. F. Monteiro, F.R.M. Lima, D.C. Moreira, D.A. Sousa, T.F. Maciel, B. Makki, H. Hannu, Paving the way toward mobile IAB: Problems, solutions and challenges, IEEE Open J. Commun. Soc. 3 (2022) 2347–2379, http://dx.doi.org/10.1109/OJCOMS.2022.3224576.

[8] A. Guidotti, A. Vanelli-Coralli, M. Conti, S. Andrenacci, S. Chatzinotas, N. Maturo, B. Evans, A. Awoseyila, A. Ugolini, T. Foggi, L. Gaudio, N. Alagha, S. Cioni, Architectures and key technical challenges for 5G systems incorporating satellites, IEEE Trans. Veh. Technol. 68 (3) (2019) 2624–2639, http://dx.doi.org/10.1109/TVT.2019.2895263.

[9] G. Sciddurlo, A. Petrosino, M. Quadrini, C. Roseti, D. Striccoli, F. Zampognaro, M. Luglio, S. Perticaroli, A. Mosca, F. Lombardi, I. Micheli, A. Ornatelli, V. Schena, A.D. Mezza, A. Mattioni, D. Morbidelli, G. Boggia, G. Piro, Looking at NB-IoT over LEO satellite systems: Design and evaluation of a service-oriented solution, IEEE Internet Things J. 9 (16) (2022) 14952–14964, http://dx.doi.org/10.1109/JIOT.2021.3135060.

[10] G. Kwon, W. Shin, A. Conti, W.C. Lindsey, M.Z. Win, Joint beamforming and resource allocation for integrated satellite-terrestrial networks, in: ICC 2023 - IEEE International Conference on Communications, 2023, pp. 2129–2134, http://dx.doi.org/10.1109/ICC45041.2023.10278943.

[11] G. Lee, J.-B. Kim, A network architecture of NOMA-cdrt based on 3GPP new radio standards, in: 2023 14th International Conference on Information and Communication Technology Convergence, ICTC, 2023, pp. 1614–1616, http://dx.doi.org/10.1109/ICTC58733.2023.10392636.

[12] M. Sheng, Y. Zhang, J. Liu, Z. Xie, T.Q.S. Quek, J. Li, Enabling integrated access and backhaul in dynamic aerial-terrestrial networks for coverage enhancement, IEEE Trans. Wireless Commun. (2024) 1, http://dx.doi.org/10.1109/TWC.2024.3358296.

[13] Z. Lou, B.E. Youcef Belmekki, M.-S. Alouini, HAPS in the non-terrestrial network nexus: Prospective architectures and performance insights, IEEE Wirel. Commun. 30 (6) (2023) 52–58, http://dx.doi.org/10.1109/MWC.004.2300198.

[14] 3rd Generation Partnership Project, Study On New Radio Access Technology: Radio Access Architecture and Interfaces (Release 14), TS 38.801, 2017, (Online Accessed 14 March 2024).

[15] A. Bishen, Innovations in 5G backhaul technologies — 5gamericas.org, 2020, https://www.5gamericas.org/innovations-in-5g-backhaul-technologies/. (Online Accessed 14 March 2024).

[16] 3rd Generation Partnership Project, Study on Integrated Access and Backhaul (Rel16), TS 38.874, 2019, (Online Accessed 14 March 2024).

[17] 3rd Generation Partnership Project, NR; Backhaul Adaptation Protocol (BAP) Specification, TS 38.340, 2023, (Online Accessed 14 March 2024).

[18] 3rd Generation Partnership Project, Integrated Access and Backhaul Radio Transmission and Reception, TS 38.174, 2023, (Online Accessed 14 March 2024).

[19] 3rd Generation Partnership Project, Study on New Radio (NR) To Support Non-Terrestrial Networks (Ntns), TS 38.811, 2020, (Online Accessed 14 March 2024).

[20] 3rd Generation Partnership Project, Satellite Access Node Radio Transmission and Reception (Rel17), TS 38.108, 2024, (Online Accessed 14 March 2024).

[21] J. Christensen, ITU regulations for ka-band satellite networks, in: 30th AIAA International Communications Satellite System Conference, ICSSC, 2012, p. 15179.

[22] I.T. Union, Radio regulations appendices, 2020, (Online Accessed 14 March 2024).

[23] 3rd Generation Partnership Project, Study on Vehicle-Mounted Relays, TS 22.839, 2021, (Online Accessed 14 March 2024).

[24] 3rd Generation Partnership Project, 5G;ng-ran; architecture description, TS 38.401, 2023, (Online Accessed 14 March 2024).

[25] 3rd Generation Partnership Project, Radio Resource Control (RRC);, TS 38.331, 2023, (Online Accessed 14 March 2024).

[26] S. Martiradonna, A. Grassi, G. Piro, G. Boggia, Understanding the 5G-air-simulator: A tutorial on design criteria, technical components, and reference use cases, Comput. Netw. 177 (2020) 107314, http://dx.doi.org/10.1016/j.comnet.2020.107314.

[27] 3rd Generation Partnership Project, Physical Layer Procedures for Control, TS 38.213, 2024, (Online Accessed 11 June 2024).

[28] 3rd Generation Partnership Project, NR; Base Station (BS) Radio Transmission and Reception, TS 38.104, tbd, (Online Accessed 14 March 2024).

[29] L. Ippolito, Satellite Communications Systems Engineering: Atmospheric Effects, Satellite Link Design and System Performance, Wiley, 2017, http://dx.doi.org/10.1002/9781119259411.

[30] C.A. Balanis, Antenna Theory: Analysis and Design, second ed., Wiley, 1996.
[31] M.A. Wibisono, A. Mustafa, Iskandar, Hendrawan, T. Juhana, A. Munir, Automatic VSAT antenna pointing system featured with non-horizontal alignment autocorrect, in: 2017 7th International Annual Engineering Seminar (InAES), 2017, pp. 1–4, http://dx.doi.org/10.1109/INAES.2017.8068543.
[32] 3rd Generation Partnership Project, Physical Layer Procedures for Data, TS 38.214, 2023, (Online Accessed 14 March 2024).
[33] free5GC, 2024, https://github.com/free5gc/free5gc. (Online Accessed 14 March 2024).
[34] UERANSIM, 2024, https://github.com/aligungr/UERANSIM. (Online Accessed 14 March 2024).

**Daniele Pugliese** received a Bachelor's Degree in Computer and Automation Engineering and a Master's Degree in Telecommunication Engineering (both cum laude) from Politecnico di Bari in 2021 and 2023, respectively. His interests range from technologies supporting Beyond 5G and 6G mobile systems, such as Smart Radio Environments and Non-Terrestrial Networks, to network security. Since November 2023 he is a Ph.D. Student in Smart and Sustainable Industry at the Department of Electrical and Information Engineering, Politecnico di Bari.

**Mattia Quadrini** is currently employed as Internet Engineer in the R&D Department at Romars. He received the Ph.D. in Electronic Engineering at University of Rome "Tor Vergata" in 2023, and his MS degree cum laude in ICT and Internet Engineering, in 2019. He is involved in research activities focused on satellite communications, design of network virtualization technologies, analysis of 3GPP specifications and ETSI standards.

**Domenico Striccoli** received, with honors, the Dr. Eng. Degree in Electronic Engineering in April 2000, and the Ph.D. degree in April 2004, both from the Politecnico di Bari, Italy. In 2005 he joined the DIASS Department of Politecnico di Bari in Taranto as Assistant Professor in Telecommunications. Actually he teaches fundamental courses in the field of Telecommunications at Department of Electrical and Information Engineering (DEI) of Politecnico di Bari, where he holds the position of Assistant Professor in Telecommunications. Dr. Striccoli has authored numerous scientific papers on various topics related to electronic engineering. His work has been published in esteemed international journals and presented at leading scientific conferences.

**Cesare Roseti** is currently Associate Professor in Computer Science at the University of Rome "Tor Vergata". He graduated cum laude in 2003 in Telecommunication Engineering and received the Ph.D. degree in "Space systems and technologies" in 2007 at University of Rome "Tor Vergata". In 2003 and 2004, he was a visiting student at Computer Science Department of University of California, Los Angeles (UCLA). In 2005 he collaborated as a trainee at the TEC-SWS division of the European Space Agency (Noordwijk, The Netherlands). In 2009, he achieved II-level master on "Homeland Security" at the University of Bologna. He teaches "Broadcast and Multimedia technologies" and "Security of Internet infrastructures" in the ICT and Internet Engineering course, at the University of Rome "Tor Vergata". He is involved in national and international research projects in the ICT field, playing the role of technical and project manager. Finally, he is co-author of more than 100 indexed scientific publications.

**Francesco Zampognaro** is currently Associate Professor at the Link Campus University. He has received the Ph.D. in Space Systems and Technologies from the University of Rome "Tor Vergata" and the M.Sc. in Telecommunication Engineering from the University of Rome "La Sapienza". He is involved in teaching and research activities related to Satellite Systems, mobile networks, virtualization, TCP/IP protocols and applications, services provision and QoS, security, integrated/hybrid architectures. He is founder of the University spin-off RomARS, focusing in the provision of 5G solutions, wireless and Satellite connectivity services, and in-network functions.

**Giuseppe Piro** is an Associate Professor at "Politecnico di Bari", Italy. He received the Ph.D. degree in Electronic Engineering, a first, and a second level degree (both with Hons.) in Telecommunications Engineering from "Politecnico di Bari", Italy, in 2006 and 2008, respectively. His main research interests include wireless networks, network simulation tools, 5G and beyond, network security, nano-scale communications, Internet of Things, and Software-Defined Networking. He serves as Associate Editor for Internet Technology Letter (Wiley), Wireless Communications and Mobile Computing (Hindawi), and Sensors (MDPI).

**Luigi Alfredo Grieco** is a full professor in telecommunications at Politecnico di Bari.His research interests include Internet of Things, Future Internet Architectures, and Nano-communications. He serves as Founder Editor in Chief of the Internet Technology Letters journal (Wiley) and as Associate Editor of the IEEE Transactions on Vehicular Technology journal (for which he has been awarded as top editor in 2012, 2017, and 2020).

**Gennaro Boggia** received the Dr.Eng. and Ph.D. degrees (with Hons.) in electronics engineering from the Politecnico di Bari, Bari, Italy, in July 1997 and March 2001, respectively. He is a Full Professor of Telecommunication with the Politecnico di Bari, Bari, Italy. His research interests include wireless networking, cellular communication, protocol stacks for industrial applications and smart grids, Internet measurements, and network performance evaluation.